ANNUAL REVIEWS **Further**

Click here for quick links to Annual Reviews content online, including:

- Other articles in this volume
- Top cited articles
- Top downloaded articles
- Our comprehensive search

Annu. Rev. Marine. Sci. 2011.3:227-260. Downloaded from www.annualreviews.org
by CSIC - Consejo Superior de Investigaciones Cientificas on 11/04/11. For personal use only.

Marine Primary Production in Relation to Climate Variability and Change

Francisco P. Chavez, Monique Messié, and J. Timothy Pennington

Monterey Bay Aquarium Research Institute, Moss Landing, California 95039; email: chfr@mbari.org

Annu. Rev. Mar. Sci. 2011. 3:227–60

First published online as a Review in Advance on October 27, 2010

The *Annual Review of Marine Science* is online at marine.annualreviews.org

This article's doi: 10.1146/annurev.marine.010908.163917

Copyright © 2011 by Annual Reviews. All rights reserved

1941-1405/11/0115-0227$20.00

Keywords

primary production, climate, nutrients, phytoplankton, biogeochemistry

Abstract

Marine photosynthetic plankton are responsible for approximately 50 petagrams (10^{15}) of carbon per year of net primary production, an amount equivalent to that on land. This primary production supports essentially all life in the oceans and profoundly affects global biogeochemical cycles and climate. This review discusses the general distribution of primary production in the sea, the processes that regulate this distribution, and how marine primary production is sensitive to climate variability and change. Statistical modes of ocean variability and their characteristic interannual to multidecadal timescales over the last century are described. Recent in situ and satellite time-series of primary production can be clearly linked to interannual ocean variability. Global marine primary production appears to have increased over the past several decades in association with multi-decadal variations. A paleoclimate record extends discussion to the centennial scale, providing contrasting insights into how marine primary production might vary in the future.

Annu. Rev. Marine. Sci. 2011.3:227-260. Downloaded from www.annualreviews.org
by CSIC - Consejo Superior de Investigaciones Cientificas on 11/04/11. For personal use only.

INTRODUCTION

Sunlight, water, and plant nutrients are required to support photosynthesis, whereby oxidized inorganic carbon is converted to energy-rich organic carbon molecules, a process also termed primary production (PP). PP's chemical fixation of the sun's energy fuels essentially all life on earth and, in turn, regulates atmospheric carbon dioxide and oxygen concentrations, profoundly affecting climate and biogeochemical cycles. In the oceans, photosynthesis is conducted mainly by microscopic drifting plankton that inhabit the well-lit upper few percent of the ocean, called the euphotic zone. The remainder of the ocean is too dark to support net photosynthesis. Plant nutrients, inorganic molecules required for the synthesis and growth of cells, occur in relatively low quantities in the euphotic zone, and their rate of replenishment plays a dominant role in the regulation of marine PP. In the dark below the euphotic zone, nutrient concentrations increase (Sverdrup et al. 1942, Barber & Chavez 1983) (**Figure 1*c***) because PP-derived particulate organic matter sinks and decays at depth. This decay uses oxygen and converts the organic matter produced by PP back into nitrate, phosphate, and other plant nutrients. The process that begins with PP, is followed by the sinking of PP-derived materials down and out of the euphotic zone, and ends with decay of organic material at depth or deposition on the bottom of the ocean is termed the biological pump.

The physical processes that return nutrients to the euphotic zone vary geographically in a markedly but orderly fashion so that high- and low-PP regions are characteristic of the oceans, analogous to forests and deserts on land. The average ocean has a shallow layer of light (warm or fresh) water over a deep, denser layer, separated by a zone of strong vertical gradients in temperature and nutrients that is termed the thermocline, or nutricline. Such water column stratification prevents vertical mixing of cooler, nutrient-rich water to the euphotic zone. However, at high latitudes ($\gtrsim$40°), winter cooling and storms destabilize the water column, eroding the thermocline downwards while nutrients are mixed to the surface (**Figure 1*b***). In these areas, phytoplankton often bloom after the winter mixing season when sunlight increases and spring/summer stratification redevelops (Sverdrup 1953). In these regions, winter mixing depth dictates the quantity of nutrients available for the spring bloom and can be impacted year to year by variations or trends in wind speed and stratification. At lower latitudes, the wind-driven surface flow with the earth's rotation causes the thermocline to shoal or upwell, particularly at the margins of the subtropical gyres (Barber & Chavez 1983) (**Figure 1*a–c***). In such areas, nutrients are lifted into the euphotic zone and rates of primary production are elevated (**Figure 1*d***). In general, winter mixing and thermocline erosion dominate nutrient supply processes at high latitudes; at low latitudes, thermocline shoaling and upwelling become the main supply processes

Figure 1

Global mean sea surface height, winds, nutricline depth, and primary production. (*a*) Dynamic height, calculated from the CNES-CLS09 v1.1 product for 1993–1999 (Aviso, France); the tight contours of the fast western boundary and west wind drift currents and the subtropical gyres are clearly visible. (*b*) Mean wind speed (*colors*) with direction and speed vectors (*arrows*), calculated from the QuickSCAT monthly 25-km-resolution product for August 1999–July 2008 (Natl. Ocean. Atmos. Adm.); the higher average wind speeds at high latitudes and the steady trades are evident. (*c*) Nutricline depth, estimated as the depth where there is an increase of 1 μmolar nitrate relative to the surface, from the WOA05 climatology at **http://www.nodc.noaa.gov/OC5/WOA05/pr_woa05.html**); the shallower nutricline along coastal boundaries, the equator, and high latitudes is in contrast with the deep nutricline in the subtropical gyres. (*d*) Primary production, calculated from the VGPM SeaWIFS product for September 1997–December 2007 at **http://www.science.oregonstate.edu/ocean.productivity**. The locations of in situ time-series presented in the review are shown on the primary productivity map (*d*).

(Pennington et al. 2006). Within the subtropical gyres, where the thermocline and nutricline are stable and deep (200–300 m), phytoplankton remain strongly nutrient limited. Within such oligotrophic regions, the main nutrient supply mechanisms are (*a*) slow diffusion across the thermocline (Lewis et al. 1994, Chavez & Toggweiler 1995), (*b*) thermocline shoaling or upwelling associated with open ocean eddies (McGillicuddy et al. 1998), and (*c*) nitrogen fixation. Nitrogen fixation is a process by which dinitrogen gas from the atmosphere, rather than nitrate from the thermocline, is used by phytoplankton as a nitrogen source (Karl et al. 2002). Iron, an essential micronutrient, can also be supplied from the atmosphere via long-distance transport of continental

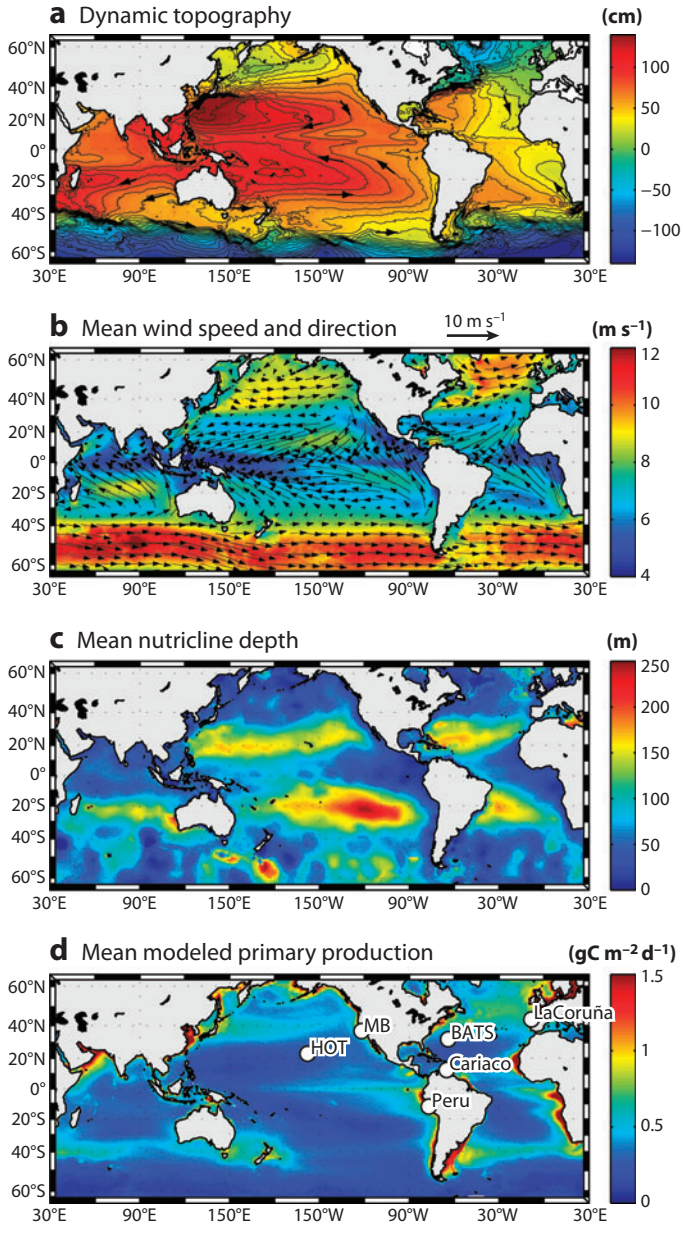

Annu. Rev. Marine. Sci. 2011.3:227-260. Downloaded from www.annualreviews.org
by CSIC - Consejo Superior de Investigaciones Cientificas on 11/04/11. For personal use only.

dust (Martin & Fitzwater 1988). Temporally, climate variability and change can impact nutrient supply and PP in the oceans. For example, El Niño causes basin-scale adjustments in the depth of the thermocline once every three to eight years, particularly in upwelling regions, and dramatically alters nutrient supply and PP regionally (Barber & Chavez 1983). The climate-driven variability of nitrogen-fixation, elucidated partly from paleoclimatic records, is linked to ocean circulation through deep ocean ventilation, oxygen consumption at depth, denitrification, and supply of excess phosphate to the surface (Galbraith et al. 2004, Deutsch et al. 2007). The atmospheric transport of iron dust is also clearly linked to climate variation.

Thus, the wind-driven circulation and mixing of the upper ocean (**Figure 1*a*,*b***) controls the depth at which nutrients increase (the nutricline usually co-occurs with the thermocline) (**Figure 1*c***), the resupply of these nutrients to the euphotic zone, and the spatial distribution of marine PP (**Figure 1*d***). On this basis, nutrient supply and PP in the oceans have been partitioned into a number of broadly defined biogeochemical provinces (Sverdrup et al. 1942; expanded on by Barber 1988, Longhurst et al. 1995, Longhurst 1998). The primary provinces are the (*a*) eastern and (*b*) western boundaries, (*c*) equatorial upwelling, (*d*) tropical and subtropical open ocean and interior subtropical gyres, (*e*) subarctic gyres, (*f*) high-latitude, seasonally deep-mixing systems (dominated spatially by the Southern Ocean), and (*g*) continental margins (Barber 1988, Chavez & Toggweiler 1995). The interior subtropical gyres, with their deep nutricline, are flanked by strong western and weaker eastern boundary currents and by equatorial and polar westerly currents (west wind drifts) (**Figure 1*a*,*c***). Upwelling of cool, nutrient-rich water from depth occurs at the edges of the gyres, particularly on their eastern and equatorial boundaries. Eastern boundary, coastal upwelling systems, where nutrient supply and primary production are high and variable, are classically thought to be low in diversity and to favor short food chains (Ryther 1969). Conversely, the subtropical gyres are less variable and have deep thermoclines, so the euphotic zone is nutrient starved, with low primary production rates and biomass and long, complex food webs (Ryther 1969, Karl et al. 1991). These two habitats represent extremes in terms of nutrient supply and primary production.

The basic thesis presented here is that spatiotemporal variations in ocean PP are controlled by nutrient supply to the euphotic zone. This straightforward thesis, however, is subject to a number of fascinating feedbacks that are not simple at all and are active areas of current research. A review and synthesis of these areas of active research starts here with general concepts and methods used to estimate ocean PP. The modern global instrumental record of sea surface temperature (SST) is then used in an analysis of the principal modes of interannual to multi-decadal climate and ocean variability. Spatiotemporal patterns from in situ and satellite time-series of PP are related to time-series of climate and ocean variability to explore the processes responsible for the observed patterns in PP. Paleoclimate studies are introduced to broaden the temporal context and lead into speculation regarding century-scale variability.

GENERAL PRINCIPLES OF PRIMARY PRODUCTION

Who Are the Primary Producers?

Photosynthesis in the ocean is conducted primarily by drifting or weakly swimming microscopic organisms, here collectively referred to as phytoplankton. Phytoplankton are composed of a broad suite of taxa, from cyanobacteria to eukaryotes, that vary considerably in size (<1 to >100 μ). Because phytoplankton live suspended in seawater along with other nonphotosynthetic organisms and particles, it is difficult to estimate phytoplankton carbon (biomass). As a result, chlorophyll, an easily measured pigment specific to photosynthesis, has become the most widely measured

Annu. Rev. Marine. Sci. 2011.3:227-260. Downloaded from www.annualreviews.org
by CSIC - Consejo Superior de Investigaciones Cientificas on 11/04/11. For personal use only.

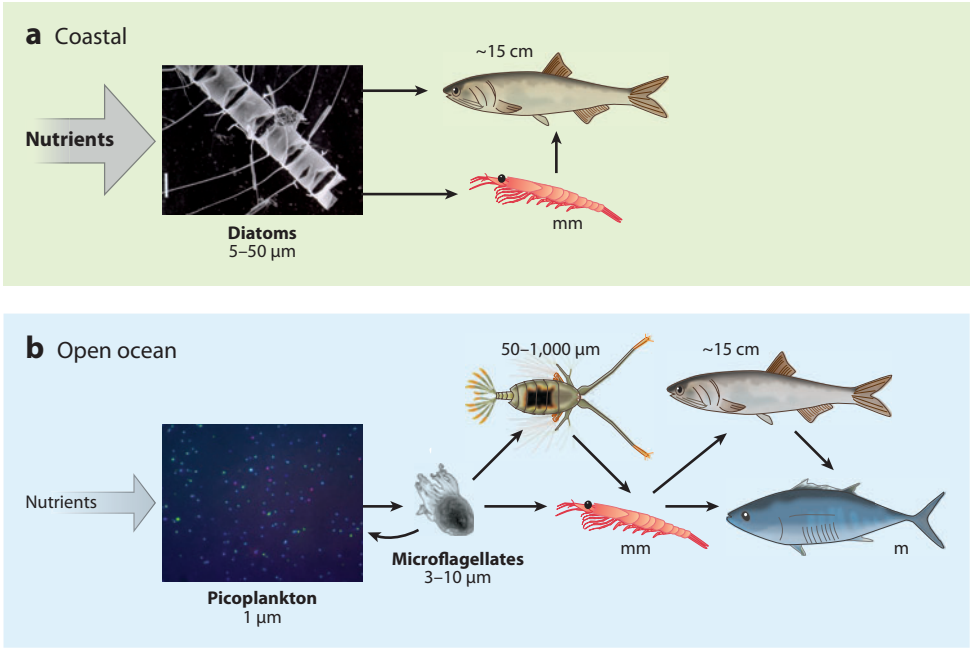

Figure 2

A conceptual model of (*a*) coastal and (*b*) open ocean pelagic ecosystems. Near coasts where nutrients are abundant, dense, colonial, centric diatom blooms form. Biomass accumulates because diatoms outgrow their macrozooplanktonic predators and primary production can be transferred rapidly to small plentiful fish. The food chain is short and efficient but leaky in that a large fraction of production is exported from the coastal upper layer. In the open ocean, under low nutrient input, photosynthetic picoplanktonic organisms dominate. The consumers of picoplankton are also very small and have growth rates similar to their prey. Scarce nutrients are recycled and retained in the upper layer. Modified from Chavez et al. (2002).

indicator of phytoplankton abundance, even though its relation to phytoplankton carbon changes significantly with light intensity, nutrient availability, and species composition (Geider 1987).

A conceptual model of pelagic ecosystems envisions two general types: eutrophic coastal and oligotrophic open ocean (Chavez et al. 2002) (**Figure 2**). Near coasts where nutrients are abundant, dense and often transient blooms of colonial centric diatoms develop. Biomass accumulates because diatoms outgrow their microbial competitors and macrozooplanktonic predators. In this coastal ecosystem, biomass can be transferred rapidly from diatoms to small, plentiful fish (Ryther 1969). Although the coastal food chain is short and thus efficient, it is also leaky in the sense that a relatively large fraction of production is often exported (Muller-Karger et al. 2005) either by sinking, where the exported production can support a rich benthic fauna or, alternately, result in anoxia (Margalef 1978), or by horizontal advection away from the coast (Olivieri & Chavez 2000, Pennington et al. 2010). In contrast, in the oligotrophic open ocean, small, photosynthetic picoplankton dominate. The grazers of picoplankton are also small and have growth rates similar to their prey. This small predator–prey community comprises the so-called microbial food web, characterized as a complex, low-nutrient input system that exports little of its production (e.g., nonleaky) (Azam et al. 1983, Pomeroy 1974) (**Figure 2**). Much fewer higher-trophic-level or fisheries resources are supported by picoplankton ecosystems because of low nutrient input, efficient internal recycling of nutrients, and the need for multiple trophic transfers to transform picoplankton production to living marine resources.

Annu. Rev. Marine. Sci. 2011.3:227-260. Downloaded from www.annualreviews.org
by CSIC - Consejo Superior de Investigaciones Cientificas on 11/04/11. For personal use only.

Annu. Rev. Marine. Sci. 2011.3:227-260. Downloaded from www.annualreviews.org
by CSIC - Consejo Superior de Investigaciones Cientificas on 11/04/11. For personal use only.

Net, Gross, and New Primary Production

This contribution focuses primarily on net primary production (NPP), which is equal to gross photosynthetic carbon fixation (or gross primary production, GPP) minus phytoplankton respiration. NPP is portion of photosynthetic carbon fixation that becomes available to the nonphotosynthetic or heterotrophic components of the ecosystem. Global marine NPP has been estimated on the order of 50 petagrams C per year (Field et al. 1998), approximately equal to the NPP of terrestrial ecosystems (Field et al. 1998, Zhao & Running 2010). Terrestrial GPP has been reported to be on the order of 120 petagrams C per year (Beer et al. 2010). The few estimates of marine GPP suggest it may also be approximately twice NPP (Bender et al. 1999). The similar GPP estimates seem odd in that marine photosynthesis is conducted mainly by microscopic, single-celled organisms, whereas terrestrial photosynthesis is conducted by complex organisms composed of roots, vascular systems, and leaves. Photorespiration in the well-lit surface layers (Corno et al. 2005) may bias marine GPP estimates.

New production (Dugdale & Goering 1967) is another climate-relevant primary production quantity. New production represents PP driven by inputs of nutrients from outside of the euphotic zone, classically taken to be nitrate (NO_3), whereas recycled production is driven by ammonium (NH_3) excreted by grazers within the euphotic zone. Nitrogen fixation is new production because the nitrogen source emanates from the atmosphere. In a euphotic zone under steady state, the import of external or new nutrients, and the eventual export of particulate organic carbon (POC) to depth—the biological pump—should be equivalent (Eppley & Peterson 1979). As phrased above, the portion of a euphotic zone's NPP that leaks to depth should, on average, be equivalent to new production and is also often referred to as net community production. Global estimates of new production vary considerably but are likely on the order of 10 petagrams carbon per year (Chavez & Toggweiler 1995), or 20% of NPP.

Light, Chlorophyll Concentration, and Euphotic Zone Integrated PP

The differences in surface chlorophyll and PP between the eutrophic and oligotrophic habitats described above can be over 2 orders of magnitude (coastal upwelling >10 mg Chl m^{-3}, >1 g C m^{-3} d^{-1}; open ocean subtropical gyres <0.05 mg Chl, <5 mg C m^{-3} d^{-1}). High surface phytoplankton biomass enhances the transport of PP to consumers but because phytoplankton and water are the primary attenuators of light in the surface ocean (Morel 1988), high surface concentrations of chlorophyll result in shallow euphotic zones. As a result, coastal and open ocean integrated chlorophyll and PP differ only by a factor of 3 to 4 (**Table 1**); the majority of global PP (80%) consequently occurs in the open ocean due to its much larger surface area. Both surface and water-column integrated chlorophyll and PP are often estimated, but integrated PP is more challenging to measure given the need to simulate growth conditions across the euphotic zone (to 1% or 0.1% surface light intensity).

Methods of Estimating PP

A diversity of methods has been developed to estimate primary production and include CO_2 fixation (Steeman-Nielsen 1952), O_2 evolution (Williams et al. 2004), nutrient uptake rate (Dugdale & Goering 1967), light capture, and electron transport measures by fluorescence (Kolber & Falkowski 1993, Kolber et al. 1998), and others. The classic and by far most commonly used method of measuring primary production is the ^{14}C-bicarbonate uptake method, as introduced by Steeman–Nielsen (1952). Water samples are spiked with a small amount of

Annu. Rev. Marine. Sci. 2011.3:227-260. Downloaded from www.annualreviews.org
by CSIC - Consejo Superior de Investigaciones Cientificas on 11/04/11. For personal use only.

Table 1 Comparison of average surface and integrated values for the open ocean and coastal time-series stations shown in Figures 1*d* and 3[a]

	BATS Open Ocean	HOT Open Ocean	La Coruña Coastal	Monterey Bay Coastal	Cariaco Coastal	Peru Coastal	Open Ocean	Coastal	Coastal/ Open Ocean
Surface primary productivity (mg C m^{-3} d^{-1})	6.7 (0.4–28, ±4.8, n = 274)	6.6 (2–25, ±2.5, n = 198)	199 (0.7–2212, ±302, n = 1,005)	140 (3.5–1481, ±165, n = 4153)	63 (3.4–814, ±85, n = 302)	143	6.7	136	20.3
Integrated PP (mg C m^{-2} d^{-1})	441 (49–1041, ±179, n = 290)	436 (154–898, ±133, n = 190)	1,713 (33–7054, ±2542, n = 205)	1,434 (126–7286, ±1,137, n = 1199)	1296 (63–6928, ±884, n = 153)	3580	437	2006	4.6
Surface chlorophyll (mg m^{-3})	0.11 (0.02–0.46, ±0.09, n = 289)	0.08 (0.03–0.23, ±0.02, n = 520)	2.4 (0.07–22, ±2.6, n = 1,244)	3.4 (0.08–26, ±3.6, n = 2,515)	0.8 (0.06–7.3, ±1.2, n = 316)	2.6	0.1	2.3	23
Integrated chlorophyll (mg m^{-2})	21 (1–66, ±10, n = 227)	18.6 (1–35, ±4.8, n = 413)	79 (5.1–317, ±75, n = 221)	59 (9.9–238, ±39, n = 1,200)	41 (11–217, ±36, n = 158)	111	13.3	72.5	5.5
Surface PP per unit chlorophyll (mg C mg chl^{-1} d^{-1})	61.9	82.6	84.5	40.9	81.6	56	72.3	65.8	0.9
Integrated PP per unit chlorophyll (mg C mg chl^{-1} d^{-1})	21	25	21.8	24.3	31.4	32.3	32.8	27.5	0.8

[a]Also shown are standard deviations, number of samples, and minima and maxima for each station/region. The BATS and HOT data were integrated to 150 m. The mean for the open ocean and coastal biomes are shown at the right with the ratio of coastal to open ocean. Coastal surface values are 20 times those of the open ocean whereas integrated values are only 3–4 times.
Abbreviations: BATS, Bermuda Atlantic Time-series Study; HOT, Hawaii Ocean Time-series; PP, primary production.

radioactive, inorganic carbon and the ^{14}C's uptake and photosynthetic conversion to reduced particulate organic carbon measured after growth in bottles. When carried out over the daylight hours, these incubations are considered NPP due to intracellular carbon refixation (Marra 2009). The method is fairly simple and apparently reliable, yet the resulting data remain subject to numerous uncertainties, the chief being suppression of productivity by low concentrations of toxins, often metals, introduced to incubations during sampling or handling (Fitzwater et al. 1982). This suppression may help explain why early ^{14}C-based global estimates were as much as 50% low (Chavez & Barber 1987; Karl et al. 2001; see Barber & Hilting 2002 for a history of global PP estimates). There are also interpretational difficulties associated with incubation. 24-hour incubations, if begun at dawn, include nighttime losses of ^{14}C via respiration. Shorter, daytime-only incubations thus produce higher uptake rates than longer, 24-hour incubations (by at least 15%; Karl et al. 1996). In spite of these complications, the ^{14}C-uptake method has been used for over almost 60 years in all the world's oceans, and the existence of such a large and fairly consistent data set provides a compelling incentive to continue its use. The estimates used in this paper are mostly derived from this technique either directly or via the satellite methods described below.

Satellite Methods

Incubation measures properties of discrete water samples, representing a square meter of the ocean. Over the past 20 years, intensive time-series programs have produced 2,037 ^{14}C integrated PP measurements (**Table 1**). As there is no repository of marine PP data, the total number of incubations remains uncertain, though it seems unlikely that more than 20,000 integrated estimates have been made. However, even if this generous figure is accepted, on average over the past 20 years, only 80 integrated ^{14}C-based PP estimates will be available annually for all the world's oceans. In contrast, a single, global 9-km resolution satellite image contains over 4 million data points (pixels), the great majority of which have never been sampled in situ. Given these limitations, the prospect of estimating PP from space is extremely attractive; daily estimates for all the world's oceans can theoretically be produced (Carr et al. 2006). A great deal of effort has thus been expended deriving algorithms that estimate NPP from satellite ocean color estimates of near-surface chlorophyll.

The satellite algorithm used here computes primary production for each pixel of ocean color–based chlorophyll using an empirical relationship between chlorophyll and near-surface P^b_{opt} (the photosynthetic carbon-uptake rate per unit chlorophyll), as adjusted by SST, and then integrated over the euphotic zone using sunlight intensity and day length (Behrenfeld & Falkowski 1997; see Friedrichs et al. 2009 and Saba et al. 2010 for a comparison of other algorithms). The P^b_{opt} versus SST relationship was developed from historical records of ^{14}C uptake, chlorophyll, and SST. Such satellite-based NPP estimates provide global coverage that cannot be achieved with in situ sampling, yet they also suffer from important inaccuracies, particularly near shore, where suspended, nonliving colored materials bias estimates. Satellite algorithms are typically applied to weekly or monthly composite data, reducing the effect of clouds and other errors, and are therefore necessarily less variable than PP data obtained by incubation. Below, we use satellite data to examine global spatial patterns of NPP over time. Satellite-based, regular global time-series of chlorophyll became available in 1997 with the launch of the Sea-viewing Wide Field-of-view Sensor (SeaWiFS; see McClain 2009 for a review of ocean color remote sensing). Earlier, the Coastal Zone Color Scanner (CZCS) operated with spotty spatial coverage over 1978–1986. A similar analysis is carried out with in situ point time-series (see time-series sites at **Figure 1*d*** and **Table 1**).

Annu. Rev. Marine. Sci. 2011.3:227-260. Downloaded from www.annualreviews.org
by CSIC - Consejo Superior de Investigaciones Cientificas on 11/04/11. For personal use only.

GLOBAL PATTERNS OF CLIMATE-DRIVEN VARIABILITY

Over the past decades, the importance of interannual and multi-decadal changes in ocean conditions and ecosystems has been recognized (Barber & Chavez 1983, Chavez et al. 2003). Marine ecologists had long noticed that ecosystems responded to subtle changes in the physical environment on interannual and longer timescales; the term regime shift was coined for these often abrupt and persistent changes in ocean ecosystems by J.D. Isaacs (1975), who first used it in reference to the rise of anchovies and fall of sardines off California in the early 1950s. Below, the results of an empirical orthogonal function (EOF) approach, developed for the analysis of North Pacific variability (Mantua et al. 1997, Zhang et al. 1997), is applied to global sea surface temperature (SST), to study the sometimes subtle changes in the physical ocean environment (M. Messié and F.P. Chavez, unpublished manuscript; see also Deser et al. 2010 for a review of the SST record). The analysis reveals well-defined patterns in the first four modes (**Figure 3**): (*a*) El Niño (McPhaden et al. 2006), (*b*) the Atlantic Multidecadal Oscillation (AMO; Kerr 2000), (*c*) the Pacific Decadal Oscillation (PDO; Mantua et al. 1997), and (*d*) the El Niño Modoki (Ashok et al. 2007) and/or the North Pacific Gyre Oscillation (Di Lorenzo el al. 2008). These patterns are described below.

Mode 1. The first EOF mode of global SST variability (M1, 17.6% of variance explained) is highly correlated to the Multivariate ENSO (El Niño Southern Oscillation) Index (MEI; Wolter & Timlin 1993; $r = 0.95$) (**Figure 3*a***). El Niño occurs every three to eight years, so the 20-year records from satellites and in situ biogeochemical time-series (see below) capture modern ENSO variations. Modern El Niño variations are further described after the remaining three modes. These variations modify the replenishment of surface nutrients to the euphotic zone through changes in the depth of the thermocline and in the direction and strength of surface winds.

Mode 2. The second mode (M2, 5.6%) has a strong North Atlantic signature (**Figure 3*b***), seems to be out of phase in the northern and southern hemispheres, and is the only mode that is not dominated by Pacific variability. The associated time-series has the longest period fluctuation among the four leading modes (order of 70 years) and is most strongly correlated ($r = 0.61$) with the AMO (**Figure 3*b***). M2 switched from negative to positive between 1995 and 2000, from positive to negative around 1970, and finally from negative to positive around 1920. The spatial pattern of M2 resembles a regression of SST anomalies on the AMO index (Deser et al. 2010) or seasonal Atlantic EOFs (Guan & Nigam 2009). Global analysis conducted by Enfield & Mestas-Nuñez (1999, 2000) identified a similar mode related to the Atlantic multi-decadal variability. The most frequently cited Atlantic climate driver is the higher-frequency North Atlantic Oscillation (NAO), but the AMO has recently emerged as a stronger driver (Frankcombe et al. 2010). The M2 spatial pattern is not as striking as those for El Niño or M3 or M4 (**Figure 3*a,c,d***). The abundance of Norwegian spring-spawning herring (Toresen & Østvedt 2000) has been linked to the AMO (Chavez 2005). A recent analysis combined the CZCS and SeaWiFS chlorophyll time-series to explore relations to the AMO and the Pacific Decadal Oscillation (Martinez et al. 2009).

Mode 3. The time-series of the third mode (M3, 4.8%) is most strongly correlated ($r = 0.60$) with the Pacific Decadal Oscillation (PDO; Mantua et al. 1997) (**Figure 3*c***). The spatial pattern of the EOF (**Figure 3*c***), however, is different from the traditional PDO pattern, which is similar to ENSO, although stronger at higher latitudes and weaker in the tropics (Mantua et al. 1997). The traditional PDO analysis (Mantua et al. 1997) includes El Niño within its first mode, but in the global analysis here, El Niño is extracted as M1 so that M3 is independent of El Niño

Annu. Rev. Marine. Sci. 2011.3:227-260. Downloaded from www.annualreviews.org
by CSIC - Consejo Superior de Investigaciones Cientificas on 11/04/11. For personal use only.

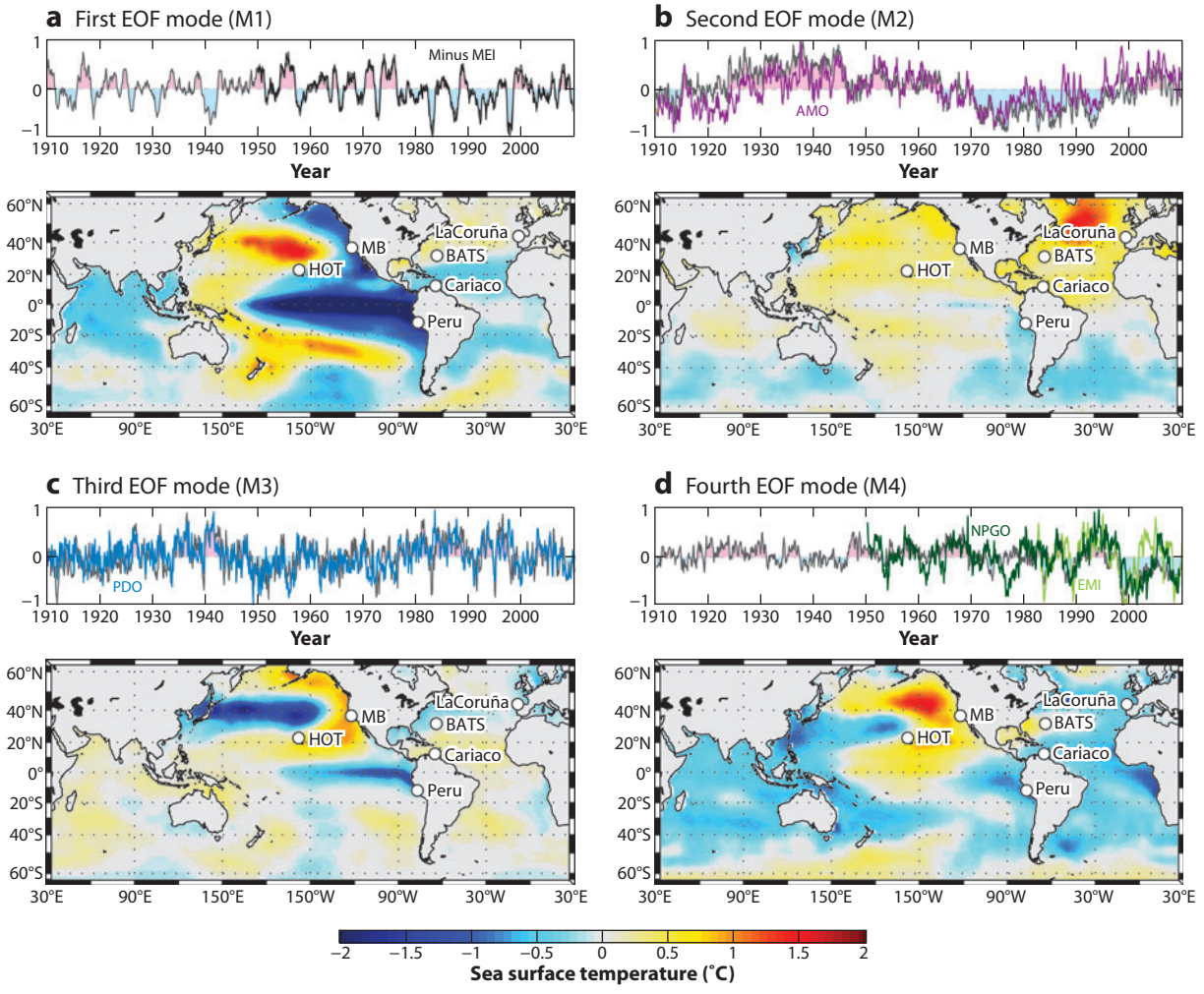

Figure 3

Empirical orthogonal function modes of global sea surface temperature (SST) with best-correlated climate indices; data from 1910–2009, trend and seasons removed, calculated from the ERSST V3b monthly product with 2° resolution for 1875–2009 at **http://www.ncdc.noaa.gov/oa/climate/research/sst/sst.php**. For each time-series, the climate index best correlated to the mode is overlain: (*a*) first EOF time-series overlain by the Multivariate El Niño Southern Oscillation (ENSO) Index (MEI, r = 0.95; **http://www.esrl.noaa.gov/psd/people/klaus.wolter/MEI/**) and first EOF spatial pattern; (*b*) second EOF time-series overlain by the Atlantic Multidecadal Oscillation (AMO, r = 0.61; **http://www.esrl.noaa.gov/psd/data/timeseries/AMO/**) and second EOF spatial pattern; (*c*) third EOF time-series overlain by the Pacific Decadal Oscillation (PDO, r = 0.60; **http://jisao.washington.edu/pdo/**) and third EOF spatial pattern; (*d*) fourth EOF time-series overlain by the El Niño Modoki (EMI, r = 0.66; Ashok et al. 2007) and North Pacific Gyre (NPGO, r = 0.57; **http://www.o3d.org/npgo/enso.html**) indices and fourth EOF spatial pattern. Modified from M. Messié and F.P. Chavez (unpublished manuscript).

and exhibits a different spatial character and a very strong North Pacific signature. The striking difference between M3 and the traditional PDO is that the northeast Pacific is out of phase with the southeastern tropical Pacific in M3. The interacting effects of modes 1 and 3 result in the traditional PDO (M. Messié and F.P. Chavez, unpublished manuscript) and drive multi-decadal changes in PP and ecosystems throughout the Pacific (Chavez et al. 2003). The strong influence of El Niño

Annu. Rev. Marine. Sci. 2011.3:227-260. Downloaded from www.annualreviews.org
by CSIC - Consejo Superior de Investigaciones Cientificas on 11/04/11. For personal use only.

on the PDO (Schneider & Cornuelle 2005) then leads to the similar spatial patterns. The M3 and PDO periodicity is on the order of 50 years, with regime shifts observed around 1925, 1945, 1976, and 1998. The current phase of M3 is for the anomalously cool and shallower thermocline in the eastern North Pacific, whereas the combined M1 and M3 adds a cool and shallower thermocline in the equatorial and southeastern tropical Pacific. The spatial pattern shows a pivot or inflection zone (separating regions of positive and negative effects) dividing the North and South Pacific basins from the western tropical Pacific to the eastern North Pacific, as does M1 (ENSO), so that the eastern and western North Pacific are out of phase (Chavez et al. 2003). The positive (warm eastern North Pacific) phase of the PDO has been associated with an intensification and eastward migration of the Aleutian Low (Mantua et al. 1997, Rodionov et al. 2005, Di Lorenzo et al. 2008), with an opposite effect (à la El Niño and La Niña) during the negative phase.

Mode 4. The fourth mode (M4, 4.5%) displays a striking warm [or cool] horseshoe-shaped pattern in the North Pacific that crosses North America around Mexico and bleeds into the western North Atlantic (**Figure 3*d***). This spatial pattern is symmetrical around the equator although, like the third mode, very diffuse in the South Pacific. The time-series of M4 is well correlated to the El Niño Modoki Index (EMI, $r = 0.66$) and the North Pacific Gyre Oscillation (NPGO, $r = 0.57$) (**Figure 3*d***). The term Modoki is Japanese for "like but not the same" and identifies warming of the western central equatorial Pacific farther west than the traditional El Niño. The EMI and NPGO indices were defined independently, the first associated with the second EOF of tropical Pacific SST (Ashok et al. 2007), and the second associated with the second EOF of sea level (or SST) for the North Pacific (Di Lorenzo et al. 2008). In the global analysis here, they combine as M4, suggesting that the two phenomena result from a single dynamical process. The periodicity of M4 seems to be more irregular but of higher-frequency (decadal) than M2 and M3. M4 indicates that the southeastern tropical Pacific cools when the western central equatorial Pacific warms. Weak coastal eastern Pacific El Niño effects have been observed when El Niño is Modoki. In contrast to the PDO, the positive (cool eastern North Pacific) phase of the NPGO has been associated with a northward Aleutian Low and a stronger than average eastern North Pacific subtropical high. This dipole acts to accelerate the North Pacific, Alaskan coastal, and California currents. The NPGO has been linked with ecosystem variations off Southern California (Di Lorenzo et al. 2008). The most striking aspect of the M4 time-series is a recent increase in amplitude with a sharp shift to negative values during 1997–1998. At the same time there has been an increase in EMI intensity (Lee & McPhaden 2010). The recent M4 phase has been amplifying the eastern North Pacific sea surface cooling and shallow thermocline condition driven by M1 and M3. Is it not clear if the M4 increase in amplitude signals the appearance of a new mode of natural variability or is related to the century-scale warming of the global ocean. How M4 and its recent trends interact with M1 and M3 needs to be elucidated.

Late 1990s climate shift. Shifts in all four modes are evident in the late 1990s. Is this coherence coincidental or the result of yet to be identified dynamical driver(s)? As a result of the coherence, the shift around 1998 may be of larger magnitude than others in the twentieth century. When trends in SST are computed over the last 30 years, a widespread cooling, driven by changes around 1998, is evident in the eastern and equatorial Pacific. The spatial character of the cooling can be clearly associated with M1, M3, and M4. This multi-decadal cooling is masked when the SST trend is calculated from 1910 (**Figure 4**). The global warming trend in SST from 1910 to 2009 (**Figure 5*a***) was removed prior to the EOF analysis discussed above; the trend's driver(s) and impact on ecosystem dynamics are of course the subject of continued debate. Solomon et al. (2010) note a decreasing trend in tropospheric temperatures after 2000, and Trenberth & Fasullo

Annu. Rev. Marine. Sci. 2011.3:227-260. Downloaded from www.annualreviews.org
by CSIC - Consejo Superior de Investigaciones Cientificas on 11/04/11. For personal use only.

Annu. Rev. Marine. Sci. 2011.3:227-260. Downloaded from www.annualreviews.org
by CSIC - Consejo Superior de Investigaciones Cientificas on 11/04/11. For personal use only.

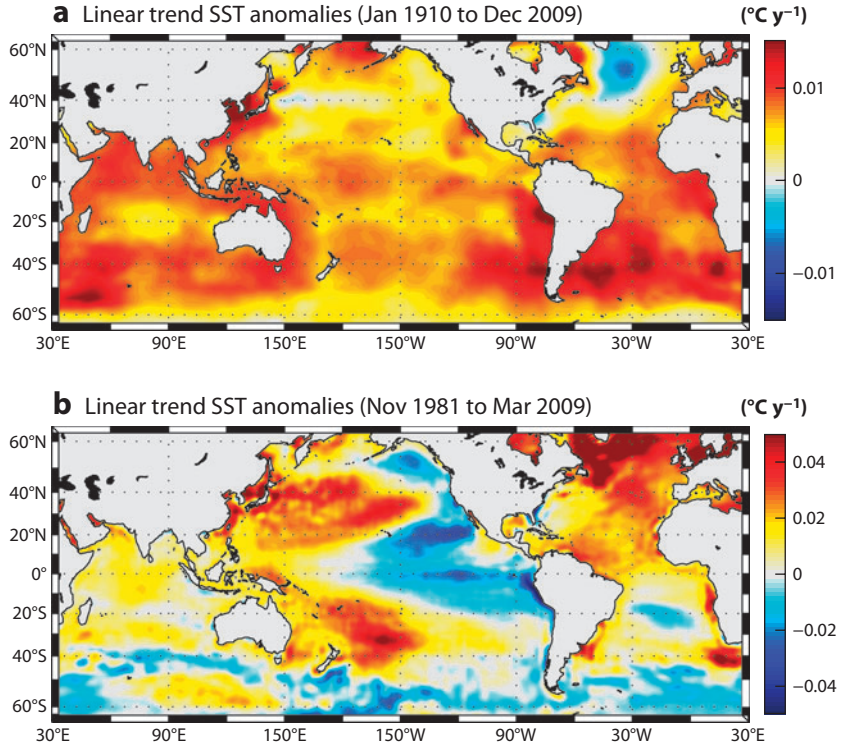

Figure 4

Global trends in sea surface temperature (SST) from (*a*) 1910–2009 using ERSST, described at **Figure 3**, and from (*b*) 1981–2009 using Reynolds et al. (2007) SST monthly averaged. Abbreviation: ERSST, extended reconstruction sea surface temperature.

(2010) show that global temperature budgets can no longer be balanced after this time. All these observations point to a major change in global environmental conditions toward the end of the twentieth century.

Interannual Variability and Biological Response: El Niño as the Dominant Mode of Climate Variability

El Niño is the strongest source of global supraseasonal ocean variability (Enfield & Mestas-Nuñez 1999, McPhaden et al. 2006, Deser et al. 2010) and produces anomalously warm SST in the equatorial and eastern Pacific every three to seven years. Anomalously cool La Niña conditions predominate between El Niños (**Figures 3*a*** and **5** show the cool eastern Pacific La Niña phase) so that SST in the equatorial and eastern Pacific is rarely average.

El Niño ("boy" or "child" in Spanish) was coined by fishermen of northern Peru in the late nineteenth century (Carranza 1891) to describe episodes when a warm poleward current became unusually strong near Christmas (the Christ Child = El Niño), even bringing crocodiles from the Guayas River in Ecuador to coastal waters off northern Peru. The warm El Niño years were also recognized to be unusually wet, with flooding and Peruvian deserts becoming grassland (Eguiguren 1894).

El Niño was related to the Southern Oscillation (ENSO for the ocean-atmosphere coupled phenomenon) during the mid-1960s (Bjerknes 1966, 1969). Sir Gilbert Walker (1924) noted that

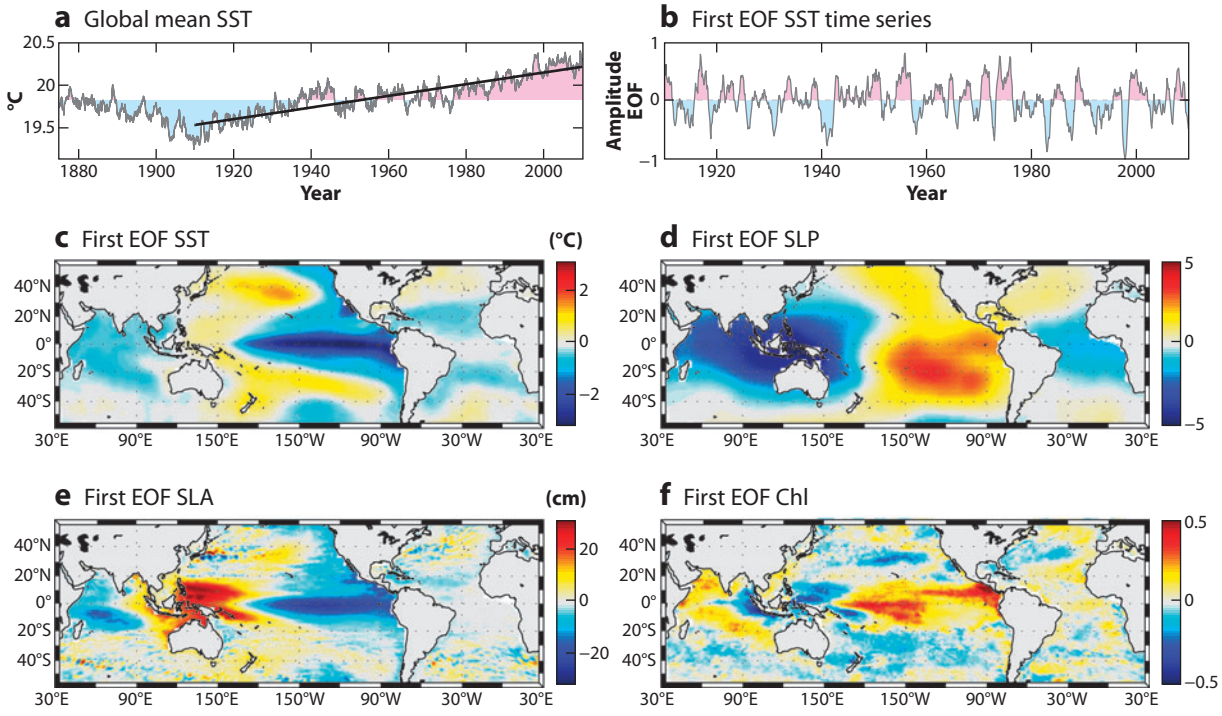

Figure 5

Global sea surface temperature (SST) and first empirical orthogonal function (EOF) modes of SST, atmospheric sea level pressure (SLP), sea level anomaly (SLA), and chlorophyll [as log(Chl)]. The cool eastern Pacific condition is represented in the EOF maps rather than the more typical warm eastern Pacific El Niño: (*a*) mean global SST time-series with seasonal cycle removed, with linear trend (*black line*) for 1910–2009 (0.0069°C y^{-1}) source as in **Figure 3**; (*b*) principal component time-series of the first EOF of 1910–2009 SST (*grey line with pink/blue fill*) after removal of the linear trend shown in (*a*); (*c*) spatial pattern of the first EOF of SST; (*d*) spatial pattern of the first EOF of SLP for 1910–2009, from the Hadley Center (HadSLP2). SLP data were normalized by dividing by latitude-specific standard deviations before the analysis; (*e*) spatial pattern of the first EOF of SLA for 1992–2008 from the Salto/Duacs reference product v2.1.0 provided by AVISO (France); (*f*) spatial pattern of the first EOF Chl for 1997–2007 from monthly SeaWiFS reprocessing 2009.1. The EOF analysis was performed on log transformed chlorophyll data. Seasonal cycles and the linear trends were removed before analysis.

when barometric pressure was high over the eastern Pacific and South America, it was low over Indonesia and Australia and vice versa and called this the Southern Oscillation (**Figure 5*d***). Compared to most tropical regions, SST in the eastern equatorial Pacific is very cool; these low SSTs are maintained by isopycnal tilting and upwelling driven by the trade winds (**Figure 1*a*,*b***). This surface water warms as it is advected across the Pacific to form the western Pacific warm pool, representing an enormous quantity of stored heat. The equatorial thermocline deepens from east to west, with cool water very close to the surface and low sea level in the east and a thick surface layer of warm water and high sea level in the west (**Figure 5*e***). The atmosphere responds to this east/west SST dipole with the Southern Oscillation's "normal" condition, wherein high pressure (dry descending air) predominates over the cool waters of the eastern Pacific, and low pressure (moist, rising air) forms over the warm western Pacific waters. The first signs of El Niño are strong westerly winds in the western Pacific between Indonesia and the date line. The western Pacific warm pool then surges eastward as a series of Kelvin waves that propagate along the equator at speeds greater than 200 km per day, raising sea level by cm and deepening the thermocline

Annu. Rev. Marine. Sci. 2011.3:227-260. Downloaded from www.annualreviews.org
by CSIC - Consejo Superior de Investigaciones Cientificas on 11/04/11. For personal use only.

by tens of meters in the east (Cane 1983, Philander 1990), creating more uniform equatorial surface temperatures, with warm water extending from Indonesia to Peru. This redistribution of heat weakens or reverses the Southern Oscillation and affects atmospheric circulation and climate worldwide (Gill & Rassmusson 1983, Rassmusson & Wallace 1983). When the Kelvin waves reach South America, they are reflected poleward along the continental margins, and El Niño is thus propagated through the ocean to mid- and high latitudes off both Americas (Enfield & Allen 1980, Enfield et al. 1987, Shaffer et al. 1997). These events take 6–18 months to play out. Recovery from El Niño leads to cooler than average La Niña conditions.

During normal conditions, upwelling of cool, nutrient-rich water from depth to the surface enhances PP in the eastern Pacific, while during El Niño nutrient supply and PP can be reduced by 80% (Barber & Chavez 1983, Chavez et al. 2002). At the same time, El Niño increases PP in the western tropical Pacific (Dandonneau 1986, Mackey et al. 1997). Changes in PP are accompanied by changes in the composition and size structure of phytoplankton that affect the entire ecosystem. During normal conditions, the diatom-dominated coastal upwelling ecosystem dominates eastern Pacific margins and the open ocean ecosystem is maintained hundreds of kilometers from shore. During El Niño, the open ocean ecosystem moves inshore to replace these normally productive waters, leaving a very narrow, high-PP coastal zone.

The strong El Niño's of 1982–1983 and 1997–1998 forcefully demonstrated that global-scale climate change can be rapid and dramatic (Chavez et al. 1999, Behrenfeld et al. 2001). Satellite time-series of chlorophyll and PP clearly show the spatiotemporal signature of El Niño (**Figures 5*f*, 6**). During La Niña, when SST and sea level are anomalously low in the eastern Pacific (and western Indian) ocean, chlorophyll is anomalously high (**Figure 5**). At the same time, SST and sea level are anomalously high in the western Pacific (and eastern Indian) and chlorophyll

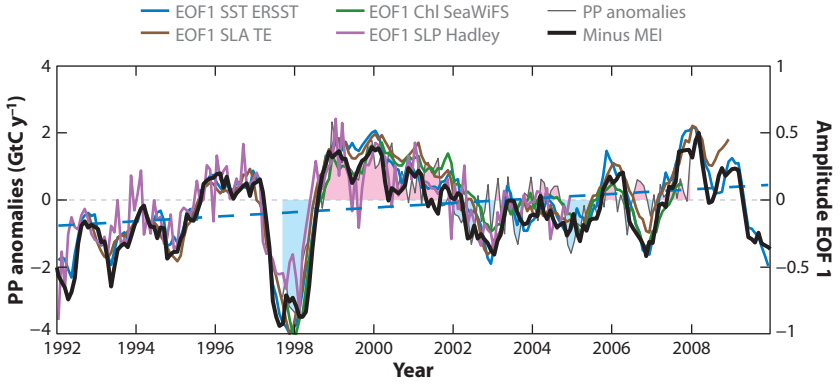

Figure 6

Global primary production anomaly (PPA) and first empirical orthogonal function (EOF) modes of sea surface temperature (SST), sea level anomaly (SLA), sea level pressure (SLP), chlorophyll (logChl), and the normalized Multivariate ENSO Index (MEI). PP anomalies were calculated as the global VGPM SeaWIFS primary production (PP) minus the 1997–2008 global mean (*thin grey line with pink/blue fill*). The first EOF modes (SST, *blue*; SLA, *brown*; SLP, *purple*; logChl, *green*) and MEI index (*black*) show high correlation with each other and PP anomalies (SST/MEI, r = 0.95; SST/SLA, r = 0.95; SST/SLP, r = 0.77; SST/Chl, r = 0.91; SST/PP, r = 0.80; SLA/MEI, r = 0.92; SLA/SLP, r = 0.81; SLA/Chl, r = 0.92; SLA/PP, r = 0.82; SLP/MEI, r = 0.79; SLP/Chl, r = 0.64; SLP/PP, r = 0.62; Chl/MEI, r = 0.0.89; Chl/PP, r = 0.80). Warm first mode SSTs are plotted as negative amplitudes, so the blue dashed line with positive slope represents a cooling trend in SST (and an increase in PP) over 1992–2009. Abbreviations: Chl, chlorophyll; SLA, sea level anomaly; SST, sea surface temperature.

Annu. Rev. Marine. Sci. 2011.3:227-260. Downloaded from www.annualreviews.org
by CSIC - Consejo Superior de Investigaciones Cientificas on 11/04/11. For personal use only.

is low. The opposite occurs during El Niño. An inflection axis or line of least variability runs from the western tropical Pacific northeast and southeast through both Pacific subtropical gyres and west wind drift regions (**Figure 5*c*,*e*,*f***). The time-series of the first EOF modes of global SST, sea level, and sea-level atmospheric pressure are highly correlated with the first modes for global chlorophyll, and PP anomalies as estimated from satellite algorithms (**Figure 6**). Behrenfeld et al. (2006) showed that for the permanently stratified surface ocean (~40°N to 40°S), satellite-derived PP was strongly correlated to the MEI. The global ocean PP anomalies show the same correlation (**Figure 6**) with greater global PP during the cool La Niña phase, indicating that increases or decreases in the eastern Pacific are not balanced by changes elsewhere. The magnitude of satellite-derived global PP interannual variability is on the order of ±2 gigatons (Gt) or petagrams (Pg) carbon per year (**Figure 6**) around a global annual mean of approximately 50 Pg C per year (Field et al. 1998). A larger negative anomaly of order 4 Pg is evident during the 1997–1998 El Niño (**Figure 6**). Equatorial Pacific variations in new PP associated with the 1997–1998 El Niño have been estimated to be 0.7 petagrams C (Chavez et al. 1999). Expanding this area to include the entire region of cooling/warming as in **Figure 4** may account for the global anomaly of ±2 petagrams (Pg) carbon per year (**Figure 6**) associated with El Niño to La Niña variations. Global marine PP, then, has varied approximately 8% annually over the last one to two decades. If the 4 Pg interannual variability primarily represents solely changes in new as opposed to recycled production, new production and nutrient supply may vary by 40% interannually. Global terrestrial NPP exhibits slightly lower interannual variability (±1 petagrams carbon, 4%; Zhao & Running 2010) but anomalies are well correlated to anomalies in the growth rate of atmospheric CO_2. For comparison, the annual global fossil fuel emission rate approximated 9 petagrams carbon per year in 2008.

Global Trends in PP

An ecosystem model simulation of the Pacific shows a spatial pattern of chlorophyll variability that is similar to that of SeaWiFS chlorophyll (**Figure 7*d*** compared with **Figure 5*f***). The simulation begins in 1991 and shows a striking regime shift after 1997–1998 (**Figure 7*c***). Observations in Monterey Bay show increases in subsurface nitrate and chlorophyll at the same time (**Figure 7*a*,*b***). The observations and the simulation are consistent with the SST analysis given above, which shows shifts in the principal modes during the same period. The ecosystem model shows that whereas regions of La Niña or La Vieja cooling have increased chlorophyll, the western half of the Pacific subtropical gyres have decreased chlorophyll (**Figure 7**), and their oligotrophic regions may be expanding, consistent with other satellite analyses (McClain et al. 2004, Gregg et al. 2005, Polovina et al. 2008).

As discussed previously, recent variations in global PP are strongly influenced by El Niño- and/or PDO-driven variation in the Pacific and result from asymmetrical impact of east–west thermocline tilt changes on the equator. In the subtropical gyres, thermocline/nutricline changes are likely also important, particularly if the thermocline pivots around the inflections described above. The nutricline in the western basins are always deep (>100 m) and will receive minimal light even if it rises (~20 m), so PP is weakly affected. However, in the east, a downward displacement of shallow nutriclines (~10 m) could strongly decrease PP. During a shallower than average eastern Pacific nutricline La Niña or La Vieja conditions PP is enhanced greater than the decrease due to a deep western Pacific nutricline. Global ocean PP is therefore higher in the deep western/shallow eastern nutricline condition. Such thermocline adjustments may occur on both interannual and decadal timescales. **Figures 6** and **7** suggest that global marine PP (and chlorophyll) has increased

Annu. Rev. Marine. Sci. 2011.3:227-260. Downloaded from www.annualreviews.org
by CSIC - Consejo Superior de Investigaciones Cientificas on 11/04/11. For personal use only.

over the past two decades and that this increase has been driven by shifts in the principal modes of multi-decadal variability (**Figure 3**).

IN SITU TIME-SERIES

At present, there are a handful of coastal and open ocean sites where physical, chemical, biological, and geological processes are being related over time. These 20-odd-year time-series programs

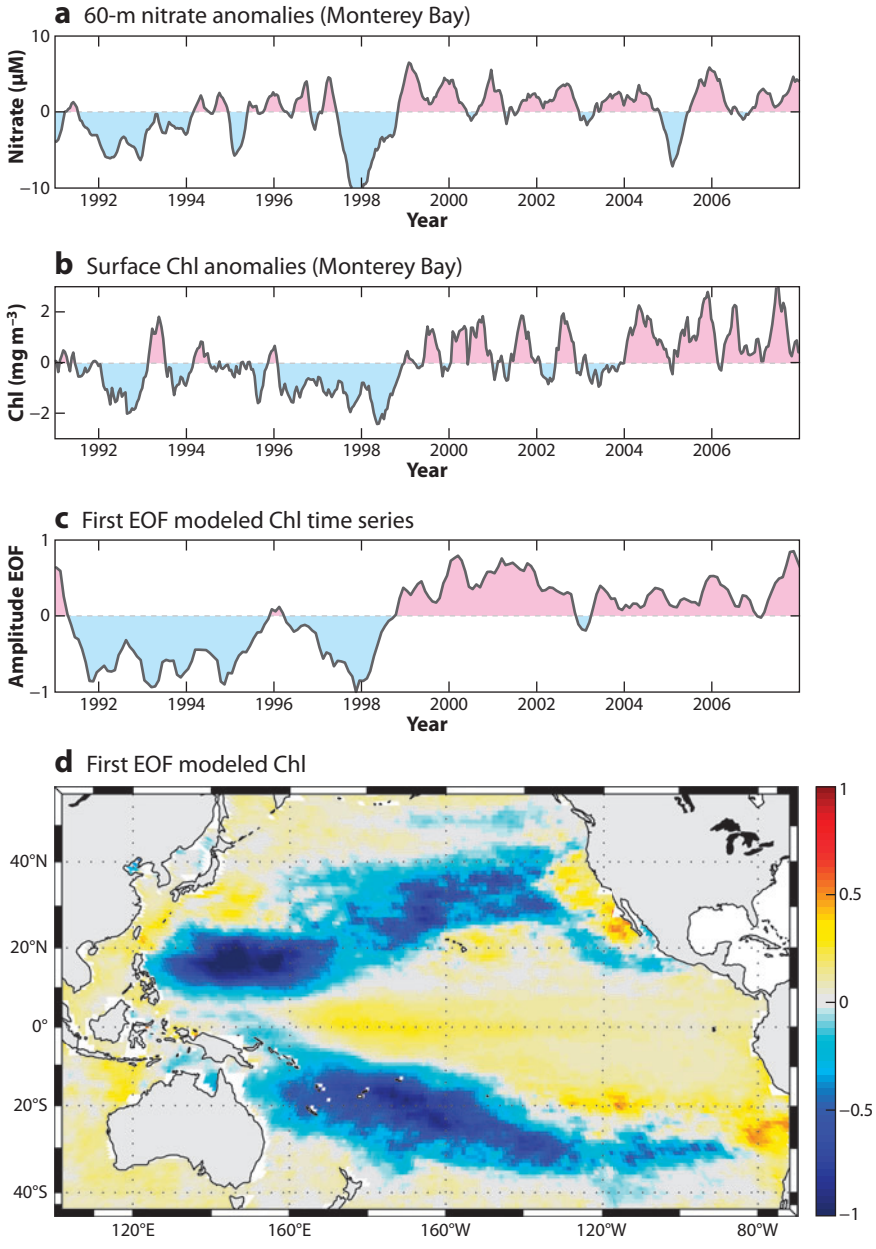

Annu. Rev. Marine. Sci. 2011.3:227-260. Downloaded from www.annualreviews.org
by CSIC - Consejo Superior de Investigaciones Cientificas on 11/04/11. For personal use only.

document variability, support process studies, methods, and technology development, provide contextual data against which short-term observations can be leveraged, and complement globally distributed observations made by satellites and other autonomous sensing platforms that measure limited sets of variables. Variations observed at the time-series are driven by a combination of local and large-scale processes, both of which are often of interest. In the following sections, the seasonal and interannual variations in chlorophyll and primary production at open ocean (Hawaii and Bermuda) and coastal (Spain, California, Venezuela, and Peru) time-series locations are reviewed in relation to larger-scale dynamics. The seasonal cycles provide information on the processes regulating PP. Time-series studies of the dynamics and feedbacks in west wind drifts and high-latitude systems are sorely missing, especially given predictions for enhanced PP in these regions due to increased stratification and reduced deep mixing, more ice-free area, and longer growing seasons. Below, we provide a brief description of each site. The sites have similar sampling schedules ranging from biweekly to monthly.

Annu. Rev. Marine. Sci. 2011.3:227-260. Downloaded from www.annualreviews.org
by CSIC - Consejo Superior de Investigaciones Cientificas on 11/04/11. For personal use only.

Coastal and Open Ocean Time-Series

North Atlantic Subtropical Gyre, BATS (31° 50′N, 64° 10′W; http://bats.bios.edu). The Bermuda Atlantic Time-series Study (BATS) samples at monthly intervals the open ocean 60 km southeast of Bermuda in the Sargasso Sea. Station S, closer to Bermuda, was first sampled in 1954 and is presently occupied as part of BATS, which began in 1988 with U.S. National Science Foundation (NSF) support for the Joint Global Ocean Flux Study (JGOFS) (as HOT below). The goals have been to construct time-series of the physics, biology, and associated biogeochemical fluxes in oligotrophic subtropical gyre waters (**Figure 1**). BATS is influenced by winter mixing but in the summer becomes fully oligotrophic (see Michaels & Knap 1996 for an overview of BATS).

North Pacific Subtropical Gyre, HOT (22° 45′N, 158°W; http://hahana.soest.hawaii.edu/hot/hot-dogs/interface.html). The Hawaii Ocean Time-series (HOT) station ALOHA, in the open ocean 100 km north of Oahu, has been occupied monthly since 1988 (as BATS above). HOT, in oligotrophic North Pacific Subtropical Gyre (NPSG) waters (**Figures 1*d***, **3**), and BATS provide contrasting Atlantic/Pacific time-series. The seasonal cycle of PP at HOT primarily reflects the annual cycle of solar irradiance. Karl et al. (2001) have suggested a cascade of influences on HOT PP by El Niño and the PDO (see Karl & Lukas 1996 for a detailed overview of HOT).

Figure 7

Time-series (1991–2008) of nitrate at 60 m (*a*) and surface chlorophyll anomalies (*b*) from Monterey Bay, Calif., compared with time-series of first empirical orthogonal function (EOF) of modeled chlorophyll (*c*) using the Regional Ocean Modeling System with an embedded nutrient, phytoplankton, zooplankton (NPZ) ecosystem (Chai et al. 2003). The spatial EOF pattern of modeled chlorophyll (*d*) can be compared with the SeaWiFS first mode of **Figure 5*f*** and shows the model domain. The EOF analysis was performed on log transformed model chlorophyll. There is strong correspondence between the Monterey Bay time-series, SeaWiFS, and the chlorophyll model results. A nutrient-driven shift in chlorophyll is evident after 1997–1998. The ROMS simulations were carried out by Fei Chai (University of Maine) and Yi Chao (NASA/JPL) as part of the Forecasting Anchovy and Sardine Transitions (FAST) project (**http://www.mbari.org/bog/fast**).

Northwestern Spain, La Coruña (43° 25.2′N, 8° 26.4′E; http://www.seriestemporales-ieo.net). Off the coast of Galicia in northwestern Spain, La Coruña station is located in a region of strong summer upwelling but where deep estuaries (rias) indent the coastline. Northerly winds favorable to upwelling predominate from April to September (Fraga 1981), whereas winter storms and southerly winds drive downwelling and mixing. At 43°N, there is a strong seasonal cycle in irradiance. Ecosystem variability has been related to the NAO with mixed results (Bode et al. 2009). The program is carried out by scientists from the Instituto Español de Oceanografia with primary funding from the Spanish government.

Central California Current (37°N, 122°W; http://www.mbari.org/bog). Physical, chemical, and phytoplankton time-series data have been collected intermittently in and off Monterey Bay, central California, beginning in 1928 (reviewed by Pennington & Chavez 2000). In 1988, the Monterey Bay Aquarium Research Institute reactivated and expanded these earlier time-series and has occupied Monterey Bay stations at two- to three-week intervals through the present. The goal is to measure the mean and fluctuating components of the pelagic ecosystem and determine the physical, chemical, and biological drivers in an eastern boundary upwelling system. Similar to La Coruña, central California seasonality is driven by spring and summer upwelling (Pennington & Chavez 2000); the region is strongly influenced by El Niño (Chavez et al. 2002) and multi-decadal variability (Chavez et al. 2003). The program is funded by the David and Lucile Packard Foundation thorough allocations to the Monterey Bay Aquarium Research Institute.

Caribbean, Cariaco Basin, Venezuela (10°30′N, 64°40′W; http://www.imars.usf.edu/CAR/index.html). Coastal upwelling occurs in the Cariaco basin during the northern hemisphere winter and spring, enhancing PP (Muller-Karger et al. 2001, 2004). This upwelling is driven by seasonal tradewinds. In summer and fall, upwelling ceases when the Inter Tropical Convergence Zone (ITCZ) region of light winds moves northward over the basin. Deep waters of the basin are anoxic year round. The presence of anoxic laminated sediments beneath a coastal upwelling region renders the Cariaco Basin of great interest to paleoclimatologists, a feature also shared with the site discussed below. The Cariaco time-series is supported by NSF, NASA, and the Venezuelan government. Ramon Varela from the Fundacion La Salle de Ciencias Naturales de Venezuela is responsible for the chlorophyll and PP data.

Coastal Peru (4–14°S; http://www.imarpe.gob.pe). The coastal ocean off Peru (to 100 km offshore) has been sampled intensively, and an integrated time-series of chlorophyll has been assembled. Although there is no PP time-series, mean values from Pennington et al. (2006) are used in **Table 1**. The coastal upwelling system off Peru is very broad (due to low latitude), experiences nearly continuous upwelling, is extremely productive in terms of fish (Chavez et al. 2008, Chavez & Messié 2009), and overlies the most intense and shallow oxygen minimum zone in the world. Paleoclimatic cores from the Peruvian continental slope are providing new links to the past and potential examples for the future (Gutierrez et al. 2009). The Peru chlorophyll time-series has been compiled from many sources but the primary is the Instituto del Mar del Peru.

Mean and Seasonal Dynamics

The mean 20-year values (**Table 1**) of the two open ocean stations are similar, although as shown in **Figure 8** they have different seasonal dynamics. The coastal stations display greater differences, with La Coruña and Monterey Bay being more productive on average than Cariaco. At the surface, the coastal sites have approximately 20 times more PP and chlorophyll than the open ocean. This

Annu. Rev. Marine. Sci. 2011.3:227-260. Downloaded from www.annualreviews.org
by CSIC - Consejo Superior de Investigaciones Cientificas on 11/04/11. For personal use only.

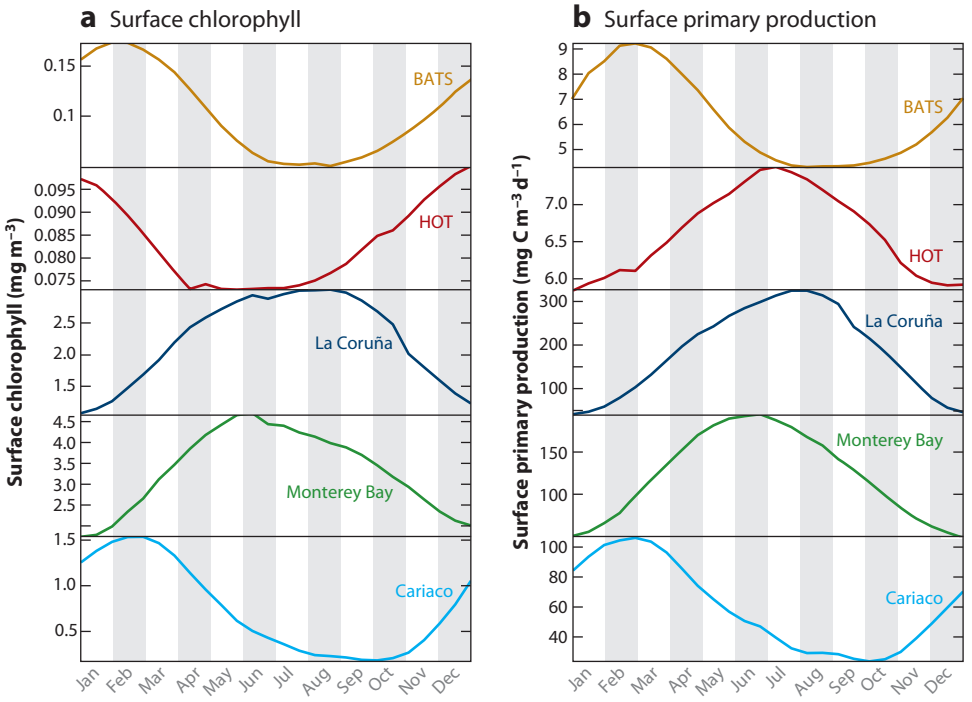

Figure 8

Surface chlorophyll (Chl; panel *a*) and seasonal surface primary production (PP; panel *b*) for the time-series sites shown in **Figures 1** and **3**. From top to bottom, panels represent the Bermuda Atlantic Time-series Study (BATS; **http://www.bios.edu/research/bats.html**); the Hawaii Ocean Time-series (HOT; **http://hahana.soest.hawaii.edu/hot/**); La Coruña, Spain (**http://www.seriestemporales-ieo.net**); the Monterey Bay Time-Series (**http://www.mbari.org/bog/Projects/CentralCal/summary/ts_summary.htm**); and Cariaco, Venezuela (**http://www.imars.usf.edu/CAR/index.html**). No adjustments have been made for site-specific methodological differences. The multi-year time-series of both PP and Chl were interpolated to a 14-d grid, smoothed with a 9-point moving average, and collapsed into 26 semimonthly bins and plotted. The integrated values show very similar patterns. At HOT, the inverted chlorophyll and PP pattern holds down to 100 m but changes to a summer maximum when the deep chlorophyll maximum at ~120 m is included.

difference, however, decreases to three to four times more when PP (or chlorophyll) is integrated over the euphotic zone (**Table 1**). This adjustment is due to light absorption by phytoplankton, so that high biomass produces a shallow euphotic zone (100-m euphotic zone in the open ocean; 10–20-m in the coastal zone). When integrated PP is normalized to integrated chlorophyll, the differences between the coastal and open ocean sites disappear (**Table 1**). PP-to-chlorophyll ratios are remarkably constant even across habitats with differing rates and mechanisms of nutrient supply, phytoplankton sizes and taxa, and euphotic zone depths.

The time-series of integrated chlorophyll and PP in **Figure 8** have been filtered to remove higher-frequency variability and then averaged to construct the seasonal cycles. The full time-series (**Figures 9**, **10**) show the considerable variability and year-to-year differences. La Coruña and Monterey Bay show maxima in summer in phase with the seasonal upwelling cycle and solar irradiance. The Cariaco maxima are in phase with the seasonal cycle of upwelling, which is maximal in winter (almost opposite that of La Coruña and Monterey Bay).

Annu. Rev. Marine. Sci. 2011.3:227-260. Downloaded from www.annualreviews.org
by CSIC - Consejo Superior de Investigaciones Cientificas on 11/04/11. For personal use only.

Annu. Rev. Marine. Sci. 2011.3:227-260. Downloaded from www.annualreviews.org
by CSIC - Consejo Superior de Investigaciones Cientificas on 11/04/11. For personal use only.

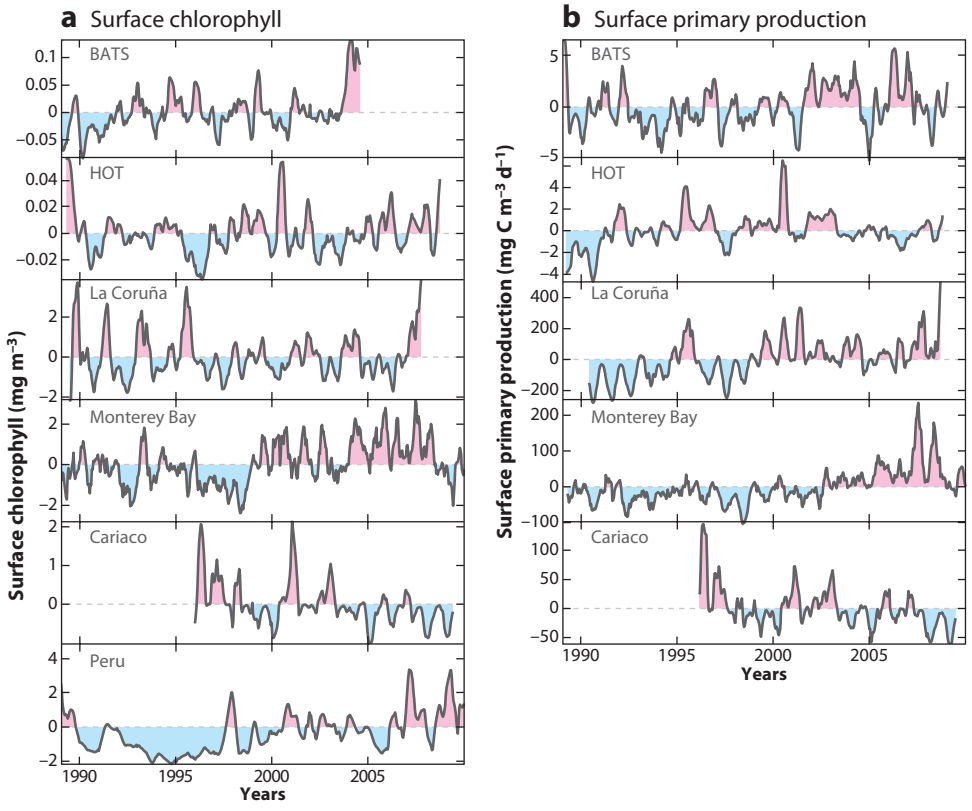

Figure 9

Time-series of surface primary production and chlorophyll anomalies for the sites shown in **Figures 1** and **3**, described at **Figure 8**. A chlorophyll series for Peru has been added here (**http://www.imarpe.gob.pe**). Anomalies were calculated by interpolating to 14 d, smoothing with a 9-point moving average, and differencing the resulting value for each 14-d interval from the grand mean for that interval. This procedure removes seasonality but not longer-scale variability or trends. (*a*) For surface primary production (PP), the 1992–1993 and 1997–1998 El Niños appear as negative (*blue*) PP anomalies at the top four sites; the years since 2000 also appear more productive (*pink*) at these four sites but not at Cariaco. (*b*) For surface chlorophyll anomalies, similar El Niño patterns may be present but only Monterey Bay appears more productive since 2000. Abbreviations: BATS, Bermuda Time-series Study; HOT, Hawaii Ocean Time-series.

The BATS seasonal cycles of PP and chlorophyll represent the classic North Atlantic pattern (reviewed by Sarmiento & Gruber 2006) of winter storm–induced downward erosion of the nutricline and upward mixing of nutrients, followed by spring thermal stratification and bloom within the euphotic zone (**Figure 8**). HOT PP is maximal in summer, in phase with the solar cycle, but the chlorophyll cycle is nearly in opposition, peaking in winter. HOT is the only site where the PP and chlorophyll cycles are not congruent. This conflict has been explained as a seasonal adjustment of cell-specific chlorophyll (Winn et al. 1995, Westberry et al. 2008). Under low winter light and deeper mixing, phytoplankton increase their per cell chlorophyll concentrations, producing the observed chlorophyll maxima. These light-induced chlorophyll adjustments apparently overwhelm the summer maximum in carbon fixation (e.g., any increase in cell number), when chlorophyll per cell is low. The deep chlorophyll maximum (DCM) increases in chlorophyll in

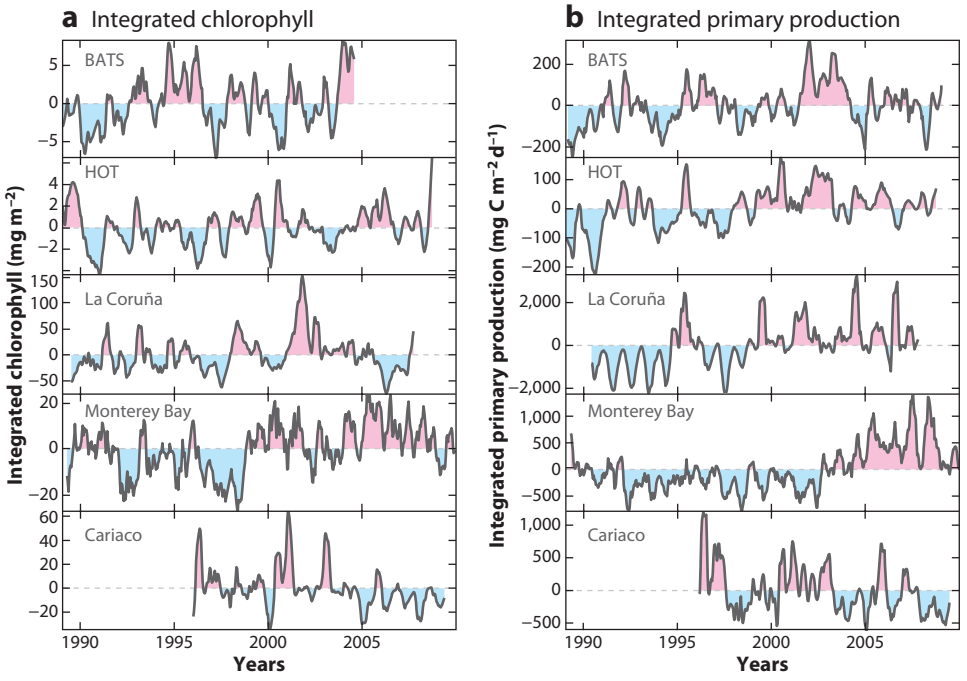

Figure 10

Time-series of water column integrated primary production (PP) and chlorophyll (Chl) anomalies for the sites shown in **Figures 1** and **3**, described at **Figure 8**. Integrated PP and Chl anomalies were calculated by integrating over the water column, then interpolating, smoothing, and differencing as described at **Figure 9**. (*a*) For PP, the 1992–1993 and 1997–1998 El Niño signals are less apparent, except perhaps at La Coruña and Monterey Bay, but all the sites except Cariaco seem to show positive (*pink*) PP anomalies after 2000. (*b*) For Chl, the 1992–1993 and 1997–1998 El Niño signals are prominent except at Cariaco.

summer at HOT (but also descends to below 100 m; Letelier et al. 2004). More light thus reaches the 100-m horizon in summer due to an increase in sunlight, a decrease in per cell chlorophyll, and a deepening of the DCM (Letelier et al. 2004).

How can the low but still substantial summer PP maximum at HOT (and the summer rates at BATS) occur in the absence of measurable nitrate? Nutrient supply and PP relationships in the subtropical gyres have been a long-running debate (Jenkins 1982, 1987; Michaels et al. 1994; Emerson et al. 1995; Karl et al. 1997). The extremely low rate of nitrate diffusion from the thermocline (Lewis et al. 1994, Chavez & Toggweiler 1995) cannot support the observed rates of euphotic zone PP. Two newly appreciated nutrient supply mechanisms at least partially resolve the questions surrounding PP nutrient support in the open ocean.

First, mesoscale eddies are common within the subtropical gyres; at a given site, passage of an eddy can produce transient shoaling of the thermocline/nutricline into the euphotic zone, increasing PP (McGillicuddy et al. 1998, 2007, and references therein). Such eddies are often missed by monthly sampling programs but appear to be most common in the spring and summer (Qiu 1999) when even moderate nutricline doming or ridging may bring nutrients into the base of the euphotic zone (Calil & Richards 2010). New profiling Argo floats with nitrate and oxygen sensors clearly show the impact of eddies at HOT (Johnson et al. 2010). However, an additional process is needed to move the eddy-pumped nutrients from the lower euphotic zone to the surface

Annu. Rev. Marine. Sci. 2011.3:227-260. Downloaded from www.annualreviews.org
by CSIC - Consejo Superior de Investigaciones Cientificas on 11/04/11. For personal use only.

20–40 m where most PP occurs. The most likely process seems to be an upward biological pump, wherein phytoplankton migrate down into the nutricline to take up nutrients (Letelier et al. 1996, Johnson et al. 2010). Similar processes likely support relatively high levels of PP at BATS in the summer, again in the absence of measurable surface nitrate.

Second, nitrogen-fixing cyanobacteria are ubiquitous in open ocean communities (Zehr & Paerl 2008) and are now recognized to leave strong imprints on ocean biogeochemistry (Gruber & Sarmiento 1997). For example, at HOT, blooms of the cyanobacterium *Trichodesmium* and the diatom *Rhizosolenia* (with symbiotic nitrogen-fixing cyanobacteria) are common in summer (Letelier et al. 2004 and references herein). These summer blooms occur in a stratified, brightly-lit euphotic zone with no measurable nitrate. Excess surface phosphorus is required but is present in the Pacific due to denitrification off the Central and South American coasts (Codispoti et al. 2001, Westberry & Siegel 2006, Deutsch et al. 2007). Nitrogen fixation is also thought to require considerable iron, which in the open ocean Pacific is likely limiting. At HOT, Asian dust and iron input is maximal in spring and early summer (Boyle et al. 2005). In the Atlantic, phosphorus and iron are supplied in Saharan dust, resulting in higher nitrogen fixation rates in the North relative to the South Atlantic (Moore et al. 2009).

Trends and Interannual to Multi-Decadal Variations

The 10–20-year series of surface and water column integrated PP and chlorophyll anomalies for the six time-series sites are shown in **Figures 9** and **10**. The large year-to-year variations are, in part, chaotic. However, close examination shows that many of the time-series capture interannual-scale variations and some resolve decadal shifts. PP and chlorophyll are increasing in 16 of the 21 time-series; the four Cariaco series and HOT surface chlorophyll have a slope of zero. At Cariaco, a decrease in winds favorable to upwelling, driven by a northward migration of the ITCZ associated with warming Atlantic and global oceans (**Figures 3*b***, **4*a***), may drive the decreasing chlorophyll and PP trends; a southward migration of the ITCZ is discussed below in association with the Little Ice Age (LIA) (Gutierrez et al. 2009, Sachs et al. 2009). The increasing trends at the Pacific sites can be related to the recent multi-decadal cooling and increased nutrient supply discussed above (Chavez & Messié 2009) (**Figure 4**). Increases at BATS and La Coruña are more difficult to interpret based on the SST EOF analysis but are supported by trends in the SeaWiFS record (not shown in the figure).

Fairly strong correspondence exists between the PP and chlorophyll series within each coastal site (La Coruña, Monterey Bay, Cariaco). Nevertheless, PP and chlorophyll are frequently decoupled. These decouplings are not surprising and can be driven by a multitude of processes including changes in species composition, carbon-to-chlorophyll ratio, growth, or solar radiation. For example, chlorophyll measured today may often better represent yesterday's PP activity. Biweekly to monthly sampling schedules are unable to capture such short-term phenomena in any case, and it has been argued that such schedules very often miss critical or controlling events. Within the subtropical gyres, the PP and chlorophyll anomalies are less obviously correlated (BATS, HOT). This lack of correspondence may be due to the cell-specific chlorophyll adjustment discussed above (in the section Mean and Seasonal Dynamics) or to generally low signal-to-noise ratios (low absolute variability) in the oligotrophic ocean (**Table 1**).

On interannual or ENSO scales, several of the time-series exhibit negative anomalies during the large 1997–1998 El Niño. In particular, surface and integrated PP at Monterey Bay and surface chlorophyll at Peru were depressed during this El Niño. Monterey Bay and Peru are sites where the first EOF mode for chlorophyll was strongly negative during this event (**Figures 5*f*, 6**). The remaining sites, however, do not show clear negative PP and chlorophyll anomalies during

Annu. Rev. Marine. Sci. 2011.3:227-260. Downloaded from www.annualreviews.org
by CSIC - Consejo Superior de Investigaciones Cientificas on 11/04/11. For personal use only.

1997–1998, and the first EOF mode for chlorophyll is near neutral at BATS, HOT, and Cariaco (**Figure 5*f***). Other variations (both positive and negative) in the observational series are not clearly associated with ENSO, although the 1992 El Niño depressed chlorophyll in Monterey Bay but not at the other sites. Karl et al. (1995) report an impact of the 1992 El Niño at HOT, although in PP and the longer time-series presented in **Figures 9** and **10**, this anomaly is not clear.

At two decades long, five of the six in situ series may be long enough to resolve decade-scale variability (Cariaco began in 1996). Qualitative evaluation of the series in **Figures 9** and **10** follow. The climate signatures in the coastal time-series are stronger given more direct connections to PP via changes in nutricline depth and local wind-driven processes that modify fluxes and stratification. Nitrogen fixation, dust deposition, and eddies are relatively unimportant to coastal PP. Coastal systems are more spatially and temporally variable than the open ocean, and this high frequency variation could mask climate change signals. However, at the open ocean sites, the combination of small absolute ranges of variability with multiple interacting processes appears to complicate relations even further. In coastal systems, strong bottom-up, nutricline-driven regulation dominates and leads to large variabilities and large-scale climate imprints.

A regime shift has been suggested following the 1997–1998 El Niño, and this shift is clearly revealed in the time-series for the first, third, and fourth EOF modes of SST variability (PDO, EMI, NPGO) (**Figure 3**). A change is also reflected in the second mode with a change of sign for the AMO (**Figure 3**). In the in situ time-series, surface and integrated chlorophyll in Monterey Bay and Peru show clear increases with this shift, although modeled chlorophyll increases over a large area after 1998 (**Figure 7*d***). Integrated PP at HOT and La Coruña also appears to increase at 1999. Bidigare et al. (2009) report a strong 1997–1998 ecosystem shift at HOT, evident in many of the HOT biogeochemical time-series, although as we have noted, weak in PP, including physical variables such as salinity (Lukas & Santiago-Mandujano 2008). HOT does tend to be near the zero-variability contour of modes 1, 3, and 4 for the North Pacific Subtropical Gyre (**Figure 3**), so the 1997–1998 shift changes may be even stronger in other open ocean Pacific locations.

THE PAST AND THE FUTURE

The SST record for the past 100 years resolves interannual- and decade-scale modes of climate variability (**Figure 3**). What drives the trend and fluctuations? What are the main feedbacks and relations between climate and ocean physics, chemistry, and biology? How will change in climate or its feedbacks affect humans? And, conversely, how will humans affect ecosystems and climate? These fundamental questions are unanswered and subject to much debate, of which this review is part. Nevertheless, great progress has been made over the past two decades due to the compilation of global data sets, models based on these data sets, and the distribution of both over the internet. Analyses of these data provide evidence for tight physical and biological coupling (SST, sea level, chlorophyll, PP) (**Figures 5**, **6**) and place strong emphasis on interannual and, more recently, decade-scale climate fluctuations. Unlike SST, biological and chemical time-series are not available for the past 100 years. However, in a few regions over strong anoxic basins without benthic macrofauna, organic and inorganic materials sink out of the water column and accumulate as layered sediments. Cores of these sediments contain an undisturbed history of the past and have been analyzed for variations in the marine nitrogen cycle, oxygen, and PP on glacial to interglacial timescales, including the LIA (~1400–1800; Galbraith et al. 2004, Gutierrez et al. 2009). Below, a recent analysis of sediment cores collected in the southeastern tropical Pacific off Peru is summarized (**Figure 11**). The purpose is to extend the discussion above to a timescale on which anthropogenic input is almost certain to affect climate.

Annu. Rev. Marine. Sci. 2011.3:227-260. Downloaded from www.annualreviews.org
by CSIC - Consejo Superior de Investigaciones Cientificas on 11/04/11. For personal use only.

Annu. Rev. Marine. Sci. 2011.3:227-260. Downloaded from www.annualreviews.org
by CSIC - Consejo Superior de Investigaciones Cientificas on 11/04/11. For personal use only.

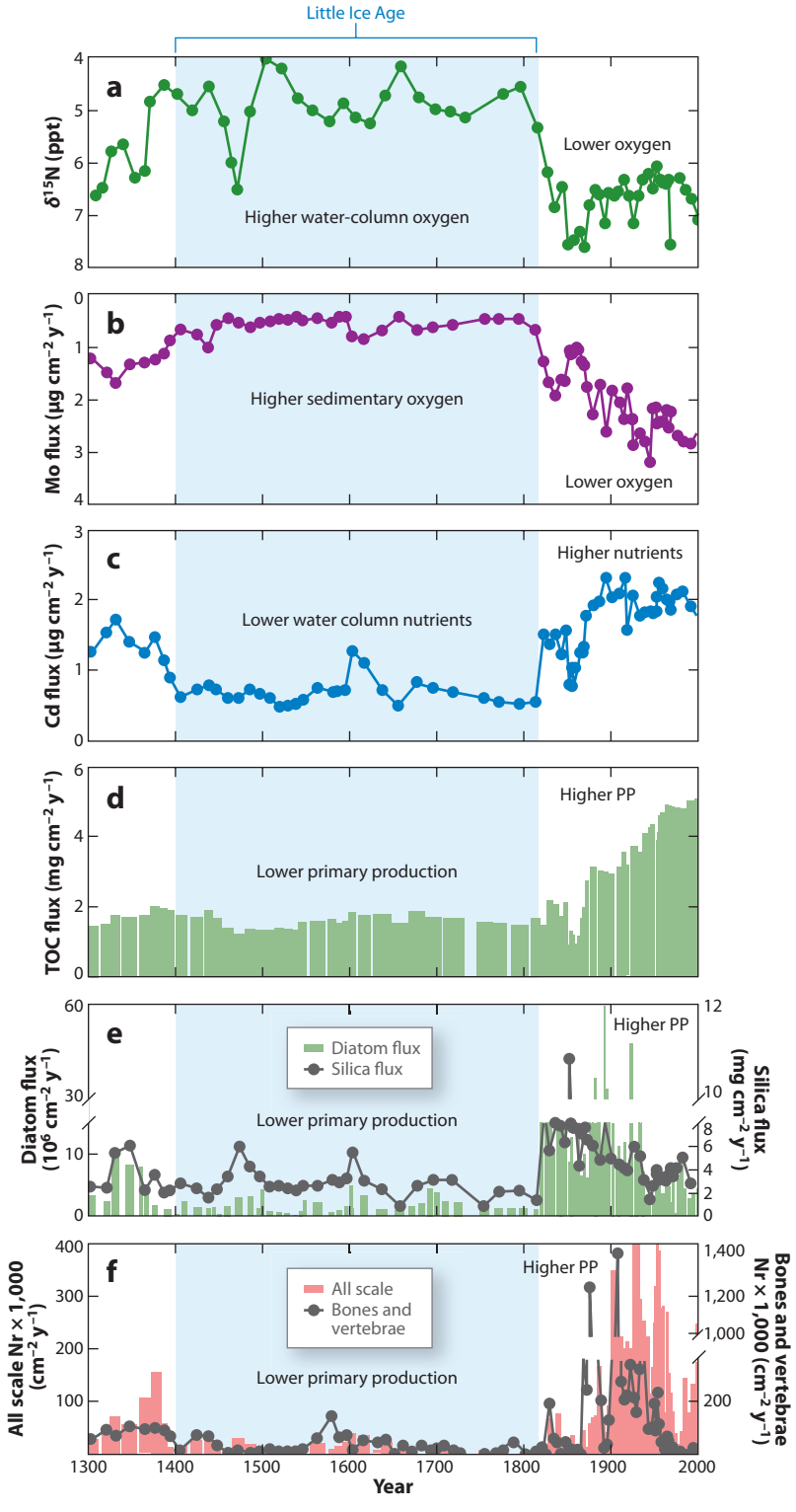

Annu. Rev. Marine. Sci. 2011.3:227-260. Downloaded from www.annualreviews.org
by CSIC - Consejo Superior de Investigaciones Cientificas on 11/04/11. For personal use only.

Relations between the marine nitrogen cycle and water column oxygen levels are relatively well understood (Broecker & Peng 1982). As water sinks at high latitudes (and in the North Atlantic in particular), and flows equatorward and to other basins, PP-derived particulate organic matter sinks and decays at depth as part of the biological pump, keeping atmospheric CO_2 levels at roughly half of what they would be otherwise (Falkowski 2002) and reducing pH at depth. The decay converts organic matter into inorganic nitrogen (mostly nitrate), phosphate, carbon, and other nutrients and uses oxygen. When water column oxygen is fully consumed in the least ventilated waters, like the eastern tropical Pacific and the Arabian Sea, decay continues with nitrate as the electron acceptor in a process called denitrification. While denitrification decreases water column nitrate, the concentrations of other nutrients continue to increase. The resulting deviation from Redfield balance (Redfield 1934) is, at present, partly rectified by nitrogen fixation in the open ocean. The timescale over which denitrification and nitrogen fixation balance occurs is uncertain (Codispoti et al. 2001), but they appear to be in phase on the timescale of ice ages (Galbraith et al. 2004); during glacial conditions, both processes are reduced in association with greater ocean ventilation.

Denitrification alters the nitrogen isotopes in sinking organic matter, and these alterations are preserved in the sediments (Altabet & Francois 1994, Galbraith et al. 2004, Gutierrez et al. 2009). Such isotopic records in the Peruvian cores indicate increased oxygenation of subsurface waters (ventilation) and decreased denitrification during the LIA (~1400–1800 AD). What drives these changes? It is thought that during the LIA an expanding northern polar ice cap pushed the ITCZ southward across the equator (Gutierrez et al. 2009, Sachs et al. 2009). Such a migration could shut down the tropical Walker circulation and, off Peru, deepen the thermocline and nutricline, increase surface layer ventilation and oxygen, decrease PP (deduced from diatom and organic carbon in cores), and lead to a sharp decline of fish (**Figure 11**). In agreement, other paleoclimate records (Mann et al. 2009) show that the equatorial Pacific cold tongue was absent during the LIA but that the preceding medieval warm period (~800–1300 AD) had an SST pattern that was very similar to the present (**Figure 3*a***) and was presumably more productive than the LIA.

The modern instrumental record shows that when the global ocean and the eastern Pacific cool during La Niña or La Vieja, global PP increases. In contrast, the sedimentary record suggests that during the LIA, when the world cooled, tropical eastern Pacific ecosystems became less productive. The post-LIA warming led to increases in eastern Pacific PP, opposite the effect of El Niño-induced warming. Scenarios that use El Niño as an analog for global warming may therefore be misleading. This conclusion has already been reached regarding tropical Pacific climate change (DiNezio et al. 2009, DiNezio & Vecchi 2010). Does it also mean that globally decreasing oxygen

Figure 11

Sediment core record from the continental slope off Callao, Peru (redrawn from Gutierrez et al. 2009): (*a*) $^{15}\delta$ N values of sedimentary organic matter (ppt), a proxy of water column oxygen; (*b*) flux of elemental molybdenum ($\mu g\ cm^{-2}\ y^{-1}$) reported by Sifeddine et al. (2008), a proxy for sedimentary oxygen levels; (*c*) flux of elemental Cadmium ($\mu g\ cm^{-2}\ y^{-1}$), a proxy of surface nutrient concentrations; (*d*) flux of total organic carbon (mg C $cm^{-2}\ y^{-1}$; Sifeddine et al. 2008), a proxy for ecosystem productivity; (*e*) bars are diatom accumulation rate (10^6 valves $cm^{-2}\ y^{-1}$) and open circles are flux of biogenic silica (mg $cm^{-2}\ y^{-1}$); proxies for production of coastal ecosystem shown in **Figure 2**; (*f*) bars are fish scale deposition rates (Nr × 1,000 $cm^{-2}\ y^{-1}$) and gray circles are deposition rates of fish bones and vertebrae (Nr × 1,000 $cm^{-2}\ y^{-1}$); proxies for production of coastal ecosystem shown in **Figure 2**. During the Little Ice Age (LIA, ~1400–1800), the ocean off Peru had high subsurface oxygen, low surface nutrients, and low primary productivity (PP), diatoms, and fish. At the end of the LIA, this condition changed abruptly to the low subsurface oxygen, eutrophic upwelling ecosystem that today produces more fish than any region of the world's oceans (Chavez et al. 2008). Abbreviations: Nr, number of remains; TOC, total organic carbon.

(and nitrate) concentrations will drive PP and fish production down? Perhaps not, as the ocean off Peru with the world's most intense oxygen minimum zone produces an order of magnitude more fish per unit PP than other upwelling regions. One wonders if the high fish yields may in fact be caused by the trapping of their zooplankton prey above shallow anoxic waters (Chavez et al. 2008, Chavez & Messié 2009).

The above results suggest that profound ocean changes have occurred over the past several centuries. Will such change continue? Certainly. Are there indications for the future? Perhaps. Decreasing oxygen and increasing nitrate have been observed in the North Pacific over the past several decades (Emerson et al. 2004, Whitney et al. 2007). Anoxia over Oregon continental shelves may be linked to higher nutrient content in upwelling source waters enhancing PP and the biological pump (Chan et al. 2008). Over larger scales globally, decreasing subsurface oxygen has been reported over the past 50 years (Stramma et al. 2008), but the processes responsible remain unresolved. The decreases could be related either to century-scale changes that started at the end of the LIA (Gutierrez et al. 2009) (**Figure 11**), multi-decadal variability of the type described by modes 1, 3, and 4 (**Figure 3**), or they could be anthropogenically driven (Gewin 2010). Recently, these factors may have acted in concert to decrease subsurface oxygen levels. Similarly, is global PP increasing due to multi-decadal changes alone, or are century-scale and anthropogenic processes also at work? Henson et al. (2010) argue that PP time-series of over 50 years will be needed before the role of anthropogenic forces can be resolved. The model results in **Figure 7** suggest that recent variations in global chlorophyll and PP (Martinez et al. 2009) and an associated expansion of the Pacific subtropical gyres (Irwin & Oliver 2009) are associated with multi-decadal variability. The general conclusions from the satellite and in situ time-series presented here are that PP is increasing globally. Available data from the Continuous Plankton Recorder surveys in the north Atlantic show increases in chlorophyll from the 1950s to the present (McQuartters-Gollop et al. 2007). However, these findings are at odds with two recent suggestions that chlorophyll is decreasing globally (Boyce et al. 2010) and that decreases in PP are further threatening fish populations under pressure from exploitation (Chassot et al. 2010). Given the paucity of data available prior to the 1980s, the sweeping conclusions of Boyce et al. (2010) are difficult to support. These opposing arguments reflect our degree of uncertainty about the directions of present and future PP change.

In coastal environments, PP, diatoms, and fish and their associated predators are predicted to decrease and the microbial food web to increase under global warming scenarios, which deepen the thermocline/nutricline or decrease its nutrient levels (see Ito et al. 2010 for a review of global change scenarios for ocean ecosystems). As discussed above, present-day trends and the sedimentary record seem to indicate that the opposite might occur. PP, however, cannot increase continuously, and feedbacks via denitrification or other processes will eventually rectify the system. When and how this will occur is complete speculation and many surprising interactions await. For example, if stratification increases but a shallow thermocline/nutricline persists, coastal dinoflagellates will increase by swimming to shallow depths to take up nutrients at night and return to the surface to photosynthesize during the day (MBARI 2007). Sedimentary records suggest that during the Paleocene, 55 million years ago, dinoflagellates were prominent along coastal margins when there were high concentrations of atmospheric CO_2 and the world was significantly warmer (Zachos et al. 2006). In open ocean subtropical gyre systems, increases in stratification are predicted to decrease nutrient supply and PP, but the picture is complicated because (*a*) multiple sources of variability are difficult to separate and characterize; (*b*) open ocean nitrate supply from the thermocline is tied to eddy activity, a phenomena poorly understood in relation to climate variability and change; (*c*) nitrogen fixation may be responsible for a large portion of new open ocean PP yet is supported by remote climate-driven processes (denitrification in the eastern boundaries) so that

Annu. Rev. Marine. Sci. 2011.3:227-260. Downloaded from www.annualreviews.org
by CSIC - Consejo Superior de Investigaciones Cientificas on 11/04/11. For personal use only.

uncertain lags are at work; (*d*) open ocean ecosystems are dependent on a climate-driven variable atmospheric iron supply, whereas coasts have a permanent source from continental shelves (Johnson et al. 1999); and (*e*) the species succession pathways among the diversity of small (0.6–10 μ), newly discovered photosynthetic plankton at the base of the open ocean food web are not well understood.

SUMMARY POINTS

1. The spatial distribution of PP reflects nutrient supply processes in the ocean. Along temperate and tropical margins, climate-driven fluctuations in the depth of the thermocline/nutricline largely control nutrient flux and PP. At high latitudes, seasonal mixing dominates. In the open ocean subtropical gyres, nutrient supply via turbulent mixing along the thermocline is amplified by mesoscale eddies and supplemented by nitrogen fixation.
2. Climate-driven fluctuations of primary production (e.g., ENSO) over the past decade and a half have been on the order of ±2 gigatons or petagrams (Pg) of carbon per year around a mean annual primary production of approximately 50 Pg. This variability is roughly 40% of new production.
3. The variability of global sea surface temperatures falls into modes that are highly correlated with well-known indices of climate variability: El Niño (ENSO), the Atlantic Multidecadal Oscillation (AMO), the Pacific Decadal Oscillation (PDO), El Niño Modoki (EM), and the North Pacific Gyre Oscillation (NPGO). Other modes and indices are sure to develop as time-series grow.
4. The drivers of the modes of climate variability and why they transition from one phase to another are mostly unknown. Some display increasing amplitudes and shifts toward the end of the last century. In particular, the equatorial and eastern Pacific has been cooler and more productive since the mid-1990s. This region drives global PP anomalies.
5. The spatial patterns of variability predict the direction and magnitude of change at particular sites. The signals are strong on the equator and on the eastern boundaries and are also strong but opposite in sign on western boundaries. The inflection between these regions (axis of zero variability) for the MEI, PDO, and EMI/NPGO passes through the subtropical gyres very near BATS and HOT.
6. Six 10–20-year in situ time-series of primary production and chlorophyll exhibit temporal variability that in some cases can be associated with the SST modes. The eastern boundary coastal sites in particular reveal the strong 1997–1998 El Niño. For the open ocean sites, PP may not be the most sensitive indicator of climate variability. Decade-scale fluctuations are less well resolved by the time-series, and there remains a great deal of unexplained variability in the anomalies.
7. Analysis of satellite and in situ time-series finds a global trend of increasing but unevenly distributed primary production.
8. Future global changes in primary production associated with global warming may not reflect the last century's SST modes (i.e., ENSO) but instead may reflect very different or even opposite century-scale warming and cooling patterns as shown by century-scale analysis of the LIA.

Annu. Rev. Marine. Sci. 2011.3:227-260. Downloaded from www.annualreviews.org
by CSIC - Consejo Superior de Investigaciones Cientificas on 11/04/11. For personal use only.

Annu. Rev. Marine. Sci. 2011.3:227-260. Downloaded from www.annualreviews.org
by CSIC - Consejo Superior de Investigaciones Cientificas on 11/04/11. For personal use only.

FUTURE ISSUES

1. The drivers of the principal modes of ocean/climate variability and their internal dynamics remain obscure.
2. Estimates by different primary production methods should be reconciled so that the relations between primary production, the principal modes of ocean/climate variability, and long term trends can be resolved. An integrated global program is recommended where community agreed–upon in situ measurements are continuously used to calibrate satellite information.
3. Relations between modes of climate fluctuation and in situ time-series are not as evident as with the satellite records and require further exploration. Additional variables should be included.
4. There is a deficiency in west wind drift and high-latitude in situ time-series.
5. Species-specific or taxon-specific primary productivity responses and resilience to climate variability and change have not been studied. It is not clear at present if coastal or open ocean ecosystems will be more resilient to climate change.
6. How important are new and yet undiscovered carbon fixation pathways that differ for traditional oxygenic photosynthesis (e.g., Zehr & Kudela 2009)?
7. The impacts of a deoxygenating subsurface ocean (Keeling et al. 2010) on denitrification, nitrogen fixation, and hence primary production cannot be accurately predicted at present.
8. The impacts of the other CO_2 problem, ocean acidification (Doney et al. 2009), on PP will need to be addressed.
9. Locally intensive in situ series, globally distributed platforms with biogeochemical sensors, and satellite information will together be needed to accurately quantify trends in marine PP as well as resolve the mechanisms behind the observed changes.

DISCLOSURE STATEMENT

The authors are not aware of any affiliations, memberships, funding, or financial holdings that might be perceived as affecting the objectivity of this review.

ACKNOWLEDGMENTS

Preparation of this review was supported by NASA and the David and Lucile Packard Foundation. We thank Reiko Michisaki for preparation of figures and tables. The dedicated work of those maintaining the time-series used and their willingness to share their data is gratefully acknowledged.

LITERATURE CITED

Altabet MA, Francois R. 1994. Sedimentary nitrogen isotopic ratio as a record for surface ocean nitrate utilization. *Glob. Biogeochem. Cycles* 8:103–16

Ashok K, Behera SK, Rao SA, Weng HY, Yamagata T. 2007. El Niño Modoki and its possible teleconnection. *J. Geophys. Res.-Oceans* 112:27

Azam F, Fenchel T, Field JG, Gray JS, Meyerreil LA, Thingstad F. 1983. The ecological role of water-column microbes in the sea. *Mar. Ecol.-Prog. Ser.* 10:257–63
Barber RT. 1988. Ocean basin ecosystems. *Ecol. Stud.* 67:171–93
Barber RT, Chavez FP. 1983. Biological consequences of El Niño. *Science* 222:1203–10
Barber RT, Hilting AK. 2002. *History of the Study of Plankton Productivity*. Oxford, UK: Blackwell
Beer C, Reichstein M, Tomelleri E, Ciais P, Jung M, et al. 2010. Terrestrial gross carbon dioxide uptake: global distribution and covariation with climate. *Science* 329:834–38
Behrenfeld MJ, Falkowski PG. 1997. Photosynthetic rates derived from satellite-based chlorophyll concentration. *Limnol. Oceanogr.* 42:1–20
Behrenfeld MJ, O'Malley RT, Siegel DA, McClain CR, Sarmiento JL, et al. 2006. Climate-driven trends in contemporary ocean productivity. *Nature* 444:752–55
Behrenfeld MJ, Randerson JT, McClain CR, Feldman GC, Los SO, et al. 2001. Biospheric primary production during an ENSO transition. *Science* 291:2594–97
Bender M, Orchado J, Dickson M, Barber R, Lindley S. 1999. In vitro O_2 fluxes compared with ^{14}C production and other rate terms during the JGOFS Equatorial Pacific experiment. *Deep-Sea Res.* I 46:637–54
Bidigare RR, Chai F, Landry MR, Lukas R, Hannides CCS, et al. 2009. Subtropical ocean ecosystem structure changes forced by North Pacific climate variations. *J. Plankton Res.* 31:1131–39
Bjerknes J. 1966. A possible response of the atmospheric Hadley circulation to equatorial anomalies of ocean temperature. *Tellus* 18:820–29
Bjerknes J. 1969. Atmospheric teleconnections from the equatorial Pacific. *Mon. Weather Rev.* 97:163–72
Bode A, Alvarez-Ossorio MT, Cabanas JM, Miranda A, Varela M. 2009. Recent trends in plankton and upwelling intensity off Galicia (NW Spain). *Prog. Oceanogr.* 83:342–50
Boyce DG, Lewis MR, Worm B. 2010. Global phytoplankton decline over the past century. *Nature* 466:591–96
Boyle EA, Bergquist BA, Kayser RA, Mahowald N. 2005. Iron, manganese, and lead at Hawaii Ocean Time-series station ALOHA: temporal variability and an intermediate water hydrothermal plume. *Geochim. Cosmochim. Acta* 69:5165–66
Broecker WS, Peng T-H. 1982. *Tracers in the Sea*. Palisades, NY: Eldigio Press. 690 pp.
Calil RHR, Richards KJ. 2010. Transient upwelling hot spots in the oligotrophic North Pacif. *J. Geophys. Res.* 115:C02003
Cane MA. 1983. Oceanographic events during El Niño. *Science* 222:1189–95
Carr ME, Friedrichs MAM, Schmeltz M, Aita MN, Antoine D, et al. 2006. A comparison of global estimates of marine primary production from ocean color. *Deep-Sea Res.* II 53:741–70
Carranza L. 1891. Contracorriente maritima observada en Payta y Pacasmayo. *Boln. Soc. Geogr. Lima* 1:344–45
Chai F, Jiang MS, Barber RT, Dugdale RC, Chao Y. 2003. Interdecadal variation of the transition zone chlorophyll front: a physical-biological model simulation between 1960 and 1990. *J. Oceanogr.* 59:461–75
Chan F, Barth JA, Lubchenco J, Kirincich A, Weeks H, et al. 2008. Emergence of anoxia in the California current large marine ecosystem. *Science* 319:920
Chassot E, Bonhommeau S, Dulvy NK, Melin F, Watson R, et al. 2010. Global marine primary production constrains fisheries catches. *Ecol. Lett.* 13:495–505
Chavez FP. 2005. Biological consequences of interannual to multidecadal variability. In *The Sea*, ed. A Robinson, K Brink, pp. 643–79. Cambridge, MA: Harvard Univ. Press
Chavez FP, Barber RT. 1987. An estimate of new production in the equatorial Pacific. *Deep-Sea Res.* I 34:1229–43
Chavez FP, Bertrand A, Guevara R, Soler P, Csirke J. 2008. The northern Humboldt Current System: brief history, present status and a view towards the future. *Prog. Oceanogr.* 79:95–105
Chavez FP, Messié M. 2009. A comparison of eastern boundary upwelling ecosystems. *Prog. Oceanogr.* 83:80–96
Chavez FP, Pennington JT, Castro CG, Ryan JP, Michisaki RP, et al. 2002. Biological and chemical consequences of the 1997–1998 El Niño in central California waters. *Prog. Oceanogr.* 54:205–32
Chavez FP, Ryan J, Lluch-Cota SE, Niquen M. 2003. From anchovies to sardines and back: multi-decadal change in the Pacific Ocean. *Science* 299:217–21
Chavez FP, Strutton PG, Friederich GE, Feely RA, Feldman GC, et al. 1999. Biological and chemical response of the equatorial Pacific Ocean to the 1997–98 El Niño. *Science* 286:2126–31

Annu. Rev. Marine. Sci. 2011.3:227-260. Downloaded from www.annualreviews.org
by CSIC - Consejo Superior de Investigaciones Cientificas on 11/04/11. For personal use only.

Chavez FP, Toggweiler JR. 1995. Physical estimates of global new production: the upwelling contribution. In *Upwelling in the Ocean: Modern Processes and Ancient Records*, ed. CP Summerhayes, KC Emeis, MV Angel, RL Smith, B Zeitzschel, pp. 313–20. Chichester, NJ: Wiley

Codispoti LA, Brandes JA, Christensen JP, Devol AH, Naqvi SWA, et al. 2001. The oceanic fixed nitrogen and nitrous oxide budgets: Moving targets as we enter the anthropocene? *Sci. Mar.* 65:85–105

Corno G, Letelier RM, Abbott MR. 2005. Assessing primary production variability in the North Pacific Subtropical Gyre: a comparison of fast repetition rate fluorometry and ^{14}C measurements. *J. Phycol.* 42:51–60

Dandonneau Y. 1986. Monitoring the sea-surface chlorophyll concentration in the tropical Pacific—consequences of the 1982–83 El-Niño. *Fish. Bull.* 84:687–95

Deser C, Alexander MA, Xie SP, Phillips AS. 2010. Sea surface temperature variability: patterns and mechanisms. *Annu. Rev. Mar. Sci.* 2:115–43

Deutsch C, Sarmiento JL, Sigman DM, Gruber N, Dunne JP. 2007. Spatial coupling of nitrogen inputs and losses in the ocean. *Nature* 445:163–67

Di Lorenzo E, Schneider N, Cobb KM, Franks PJS, Chhak K, et al. 2008. North Pacific Gyre oscillation links ocean climate and ecosystem change. *Geophys. Res. Lett.* 35:6

DiNezio PN, Clement AC, Vecchi GA, Soden BJ, Kirtman BP. 2009. Climate response of the equatorial pacific to global warming. *J. Clim.* 22:4873–92

DiNezio PN, Vecchi GA. 2010. Reconciling differing views of tropical Pacific climate change. In *EOS*, pp. 141–42. Am. Geophys. Union, Washington, DC

Doney SC, Fabry VJ, Feely RA, Kleypas JA. 2009. Ocean acidification: the other CO_2 problem. *Annu. Rev. Mar. Sci.* 1:169–92

Dugdale RC, Goering JJ. 1967. Uptake of new and regenerated forms of nitrogen in primary productivity. *Limnol. Oceanogr.* 12:196–206

Eguiguren V. 1894. Las lluvias de Piura. *Boln. Soc. Geogr. Lima* No. 4:241–58

Emerson S, Quay PD, Stump C, Wilbur D, Schudlich R. 1995. Chemical tracers of productivity and respiration in the subtropical Pacific Ocean. *J. Geophys. Res.* 100:15873–87

Emerson S, Watanabe YW, Ono T, Mecking S. 2004. Temporal trends in apparent oxygen utilization in the upper pycnocline of the North Pacific: 1980–2000. *J. Oceanogr.* 60:139–47

Enfield DB, Allen JS. 1980. On the structure and dynamics of monthly mean sea level anomalies along the Pacific coast of North and South America. *J. Phys. Oceanogr.* 10:557–78

Enfield DB, Cornejo-Rodriguez MP, Smith RL, Newberger PM. 1987. The equatorial source of propagating variability along the Peru coast during the 1982–1983 El Niño. *J. Geophys. Res.* 92:14335–46

Enfield DB, Mestas-Nunez AM. 1999. Multiscale variabilities in global sea surface temperatures and their relationships with tropospheric climate patterns. *J. Clim.* 12:2719–33

Enfield DB, Mestas-Nunz AM. 2000. Global modes of ENSO and non-ENSO SST variability and their associations with climate. In *El Niño and the Southern Oscillation: Multiscale Variability and Global and Regional Impacts*, ed. HF Diaz, V Markgraf, pp. 89–112. Cambridge, MA: Cambridge Univ. Press

Eppley RW, Peterson BJ. 1979. Particulate organic matter flux and planktonic new production in the deep ocean. *Nature* 282:677–80

Falkowski PG. 2002. The ocean's invisble forest. *Sci. Am.* 287:22, 54–56

Field CB, Behrenfeld MJ, Randerson JT, Falkowski P. 1998. Primary production of the biosphere: integrating terrestrial and oceanic components. *Science* 281:237–40

Fitzwater SE, Knauer GA, Martin JH. 1982. Metal contamination and its effects on primary production. *Limnol. Oceanogr.* 27:544–51

Fraga F. 1981. Upwelling off the Galician Coast, Northwest Spain. In *Coastal Upwelling*, ed. FA Richards. Am. Geophys. Union, Washington, DC

Frankcombe LM, von der Heydt A, Dijkstra HA. 2010. North Atlantic multidecadal climate variability: An investigation of dominant timescales and processes. *J. Clim.* 23:3626–38

Friedrichs MAM, Carr ME, Barber RT, Scardi M, Antoine D, et al. 2009. Assessing the uncertainties of model estimates of primary productivity in the tropical Pacific Ocean. *J. Mar. Syst.* 76:113–33

Galbraith ED, Kienast M, Pedersen TF, Calvert SE. 2004. Glacial-interglacial modulation of the marine nitrogen cycle by high-latitude O_2 supply to the global thermocline. *Paleoceanography* 19:12

Annu. Rev. Marine. Sci. 2011.3:227-260. Downloaded from www.annualreviews.org
by CSIC - Consejo Superior de Investigaciones Cientificas on 11/04/11. For personal use only.

Geider RJ. 1987. Light and temperature dependence of the carbon to chlorophyll a ratio in microalgae and cyanobacteria: implications for physiology and growth of phytoplankton. *New Phytol.* 106:1–34
Gewin V. 2010. Oceanography: dead in the water. *Nature* 466:821–14
Gill AE, Rasmussen EM. 1983. The 1982–83 climate anomaly in the equatorial Pacific. *Nature*: 229–34
Gregg WW, Casey NW, McClain CR. 2005. Recent trends in global ocean chlorophyll. *Geophys. Res. Lett.* 32:L03606
Gruber N, Sarmiento JL. 1997. Global patterns of marine nitrogen fixation and denitrification. *Glob. Biogeochem. Cycles* 11:235–66
Guan B, Nigam S. 2009. Analysis of Atlantic SST variability factoring interbasin links and the secular trend: clarified structure of the Atlantic Multidecadal Oscillation. *J. Clim.* 22:4228–40
Gutiérrez D, Sifeddine A, Field DB, Ortlieb L, Vargas G, et al. 2009. Rapid reorganization in ocean biogeochemistry off Peru towards the end of the Little Ice Age. *Biogeosciences* 6:835–48
Henson SA, Sarmiento JL, Dunne JP, Bopp L, Lima I, et al. 2010. Detection of anthropogenic climate change in satellite records of ocean chlorophyll and productivity. *Biogeosciences* 7:621–40
Irwin AJ, Oliver MJ. 2009. Are ocean deserts getting larger? *Geophys. Res. Lett* 36:L18609
Isaacs JD. 1975. Some ideas and frustrations about fishery science, Rep. 18, pp. 34–43. CalCOFI Report, SIO, San Diego
Ito S, Rose KA, Miller AJ, Drinkwater K, Brander K, et al. 2010. Ocean ecosystem responses to future global change scenarios: a way forward. In *Marine Ecosystems and Global Change*, ed. M Barange, R Werner, J Field, E Hofmann, pp. 410. New York: Oxford Univ. Press
Jenkins WJ. 1982. Oxygen utilization rates in North Atlantic subtropical gyre and primary production in oligotrophic systems. *Nature* 300:246–48
Jenkins WJ. 1987. ^{3}H and ^{3}He in the Beta Triangle: observations of gyre ventilation and oxygen utilization rates. *J. Phys. Oceanogr.* 17:763–83
Johnson KS, Chavez FP, Friederich GE. 1999. Continental-shelf sediment as a primary source of iron for coastal phytoplankton. *Nature* 398:697–700
Johnson KS, Riser SC, Karl DM. 2010. Nitrate supply to near-surface waters of the North Pacific subtropical gyre. *Nature* 465:1062–65
Karl D, Letelier R, Tupas L, Dore J, Christian J, Hebel R. 1997. The role of nitrogen fixation in the biogeochemical cycling in the subtropical North Pacific Ocean. *Nature* 388:533–38
Karl DM. 2002. Nutrient dynamics in the deep blue sea. *Trends Microbiol.* 10:410–18
Karl DM, Bidigare RR, Letelier RM. 2001. Long-term changes in plankton community structure and productivity in the North Pacific Subtropical Gyre: the domain shift hypothesis. *Deep-Sea Res.* II 48:1449–70
Karl DM, Christian JR, Dore JE, Hebel DV, Letelier RM, et al. 1996. Seasonal and interannual variability in primary production and particle flux at station Aloha. *Deep-Sea Res.* II 43:539–68
Karl DM, Holm-Hansen O, Taylor GT, Tien G, Bird DF. 1991. Microbial biomass and productivity in the western Bransfield Strait, Antarctica during the 1986–87 Austral summer. *Deep-Sea Res.* II 38:1029–55
Karl DM, Letelier R, Hebel D, Tupas L, Dore J, et al. 1995. Ecosystem changes in the North Pacific Subtropical Gyre attributed to the 1991–92 El-Niño. *Nature* 373:230–34
Karl DM, Lukas R. 1996. The Hawaii Ocean Time-series (HOT) program: background, rationale, and field implementation. *Deep-Sea Res.* II 43:129–56
Karl DM, Michaels A, Bergman B, Capone D, Carpenter E, et al. 2002. Dinitrogen fixation in the world's oceans. *Biogeochemistry* 57/58:47–98
Keeling RF, Kortzinger A, Gruber N. 2010. Ocean deoxygenation in a warming world. *Annu. Rev. Mar. Sci.* 2:199–229
Kerr RA. 2000. A North Atlantic climate pacemaker for the centuries. *Science* 288:1984–86
Kolber Z, Falkowski PG. 1993. Use of active fluorescence to estimate phytoplankton photosynthesis in situ. *Limnol. Oceanogr.* 38:88–106
Kolber ZS, Prasil O, Falkowski PG. 1998. Measurements of variable chlorophyll fluorescence using fast repetition rate techniques: defining methodology and experimental protocols. *Biochim. Biophys. Acta-Bioenerg.* 1367:88–106
Lee T, McPhaden MJ. 2010. Increasing intensity of El Niño in the central-equatorial Pacific. *Geophys. Res. Lett* 37:L14603

Annu. Rev. Marine. Sci. 2011.3:227-260. Downloaded from www.annualreviews.org
by CSIC - Consejo Superior de Investigaciones Cientificas on 11/04/11. For personal use only.

Letelier RM, Dore JE, Winn CD, Karl DM. 1996. Seasonal and interannual variations in phytosynthetic carbon assimilation at Station ALOHA. *Deep-Sea Res.* II 43:467–90

Letelier RM, Karl DM, Abbott MR, Bidigare RR. 2004. Light driven seasonal patterns of chlorophyll and nitrate in the lower euphotic zone of the North Pacific Subtropical Gyre. *Limnol. Oceanogr.* 49:508–19

Lewis CVW, Davis CS, Gawarkiewicz G. 1994. Wind forced biological-physical interactions on an isolated offshore bank. *Deep-Sea Res.* II 41:51–73

Longhurst AR. 1998. *Ecological Geography of the Sea*. San Diego, CA: Academic. 398 pp.

Longhurst AR, Sathyendranth S, Platt T, Caverhill C. 1995. An estimate of global primary production in the ocean from satellite radiometer data. *J. Plankton Res.* 17:1245–71

Lukas R, Santiago-Mandujano F. 2008. Interannual to interdecadal salinity variations observed near Hawaii: local and remote forcing by surface freshwater fluxes. *Oceanography* 21:56–67

Mackey DJ, Parslow J, Griffiths FB, Higgins HW, Tilbrook B. 1997. Phytoplankton productivity and the carbon cycle in the western Equatorial Pacific under El Niño and non–El Niño conditions. *Deep-Sea Res.* II 44:1951–78

Mann ME, Zhang ZH, Rutherford S, Bradley RS, Hughes MK, et al. 2009. Global signatures and dynamical origins of the little ice age and medieval climate anomaly. *Science* 326:1256–60

Mantua NJ, Hare SR, Zhang Y, Wallace JM, Francis RC. 1997. A Pacific interdecadal climate oscillation with impacts on salmon production. *Bull. Am. Meteorol. Soc.* 78:1069–79

Margalef R. 1978. What is an upwelling ecosystem? In *Upwelling Ecosystems*, ed. R Boje, M Tomczak, pp. 12–14. Berlin: Springer

Marra J. 2009. Net and gross productivity: weighing in with C-14. *Aquat. Microb. Ecol.* 56:123–31

Martin JH, Fitzwater SE. 1988. Iron deficiency limits phytoplankton growth in the North-East Pacific subartic. *Nature* 331:341–43

Martinez E, Antoine D, D'Ortenzio F, Gentili B. 2009. Climate-driven basin-scale decadal oscillations of oceanic phytoplankton. *Science* 326:1253–56

MBARI. 2007. Seeing the future in the stratified sea. Monterey Bay Aquar. Res. Inst. Annu. Rep. 2006. MBARI, Moss Landing , Calif. pp. 16–18

McClain CR. 2009. A decade of satellite ocean color observations. *Annu. Rev. Mar. Sci.* 1:19–42

McClain CR, Signorini SR, Christian JR. 2004. Subtropical gyre variability observed by ocean-color satellites. *Deep-Sea Res.* II 51:281–301

McGillicuddy DJ, Anderson LA, Bates NR, Biddy T, Buesseler KO, et al. 2007. Eddy/wind interaction stimulted extraordinary mid-ocean plankton blooms. *Science* 316:1021–27

McGillicuddy DJ, Robinson AR, Siegel DA, Jannasch HW, Johnson R, et al. 1998. Influence of mesoscale eddies on new production in the Sargasso Sea. *Nature* 394:263–66

McPhaden MJ, Zebiak SE, Glantz MH. 2006. ENSO as an integrating concept in Earth science. *Science* 314:1740–45

McQuatters-Gollop A, Raitsos DE, Edwards M, Pradhan Y, Mee LD, et al. 2007. A long-term chlorophyll data set reveals regime shift in North Sea phytoplankton biomass unconnected to nutrient trends. *Limnol. Oceanogr.* 52:635–48

Michaels AF, Bates NR, Buesseler KO, Carlson CA, Knap AH. 1994. Carbon-cycle imbalances in the Sargasso Sea. *Nature*: 537–40

Michaels AF, Knap AH. 1996. Overview of the US JGOFS Bermuda Atlantic Time-series Study and the Hydrostation S program. *Deep-Sea Res.* II 43:157–98

Moore CM, Mills MM, Achterberg EP, Geider RJ, LaRoche J, et al. 2009. Large-scale distribution of Atlantic nitrogen fixation controlled by iron availability. *Nat. Geosci.* 2:867–71

Morel A. 1988. Optical modeling of the upper ocean in relation to its biogenous content (Case I Waters). *J. Geophys. Res.* 93:10749–68

Muller-Karger F, Varela R, Thunell R, Astor Y, Zhang H, et al. 2004. Processes of coastal upwelling and carbon flux in the Cariaco Basin. *Deep-Sea Res.* II 51:927–43

Muller-Karger F, Varela R, Thunell R, Luerssen R, Hu C, Walsh JJ. 2005. The importance of continental margins in the global carbon cycle. *Geophys. Res. Lett.* 32:L01602

Annu. Rev. Marine. Sci. 2011.3:227-260. Downloaded from www.annualreviews.org
by CSIC - Consejo Superior de Investigaciones Cientificas on 11/04/11. For personal use only.

Muller-Karger F, Varela R, Thunell R, Scranton M, Bohrer R, et al. 2001. Annual cycle of primary production in the Cariaco Basin: Response to upwelling and implications for vertical export. *J. Geophys. Res.-Oceans* 106:4527–42

Olivieri RA, Chavez FP. 2000. A model of plankton dynamics for the coastal upwelling system of Monterey Bay, California. *Deep-Sea Res* II 47:1077–106

Pennington JT, Castro CG, Collins CA, Evans WWI, Friederich GE, et al. 2010. The northern and central California Coastal Upwelling System. In *Carbon and Nutrient Fluxes in Continental Margins*, ed. K-K Liu, pp. 29–44. Berlin: Springer

Pennington JT, Chavez FP. 2000. Seasonal fluctuations of temperature, salinity, nitrate, chlorophyll and primary production at station H3/M1 over 1989–1996 in Monterey Bay, California. *Deep-Sea Res.* II 47:947–73

Pennington JT, Mahoney KL, Kuwahara VS, Kolber DD, Calienes R, Chavez FP. 2006. Primary production in the eastern tropical Pacific: a review. *Prog. Oceanogr.* 69:285–317

Philander SG. 1990. *El Niño, La Niña, and the Southern Oscillation*. San Diego, CA: Academic. 289 pp.

Polovina JJ, Howell EA, Abecassis M. 2008. Ocean's least productive waters are expanding. *Geophys. Res. Lett* 35:L03618

Pomeroy LR. 1974. Oceans food web, a changing paradigm. *Bioscience* 24:499–504

Qiu B. 1999. Seasonal eddy field modulation of the North Pacific subtropical countercurrent: TOPEX/Poseidon observations and theory. *J. Phys. Oceanogr.* 29:2471–86

Rasmusson EM, Wallace JM. 1983. Meteorological aspects of El Niño/Southern Oscillation. *Science* 222:1195–201

Redfield AC. 1934. On the proportions of inorganic derivatives in sea water and their relation to the composition of plankton. In *James Johnstone Memorial Volume*, ed. RJ Daniel, pp. 177–92. Liverpool: Univ. Liverpool Press

Reynolds RW, Smith TM, Liu C, Chelton DB, Casey KS, Schlax MG. 2007. Daily high-resolution-blended analyses for sea surface temperature. *J. Clim.* 20:5473–96

Rodionov SN, Overland JE, Bond NA. 2005. Spatial and temporal variability of the Aleutian climate. *Fish. Oceanogr.* 14:3–21

Ryther JH. 1969. Photosynthesis and fish production in the sea. *Science* 166:72–76

Saba VS, Friedrichs MAM, Carr M-E, Antoine D, Armstrong RA, et al. 2010. The challenges of modeling depth-integrated marine primary productivity over multiple decades: A case study at BATS and HOT. *Glob. Biogeochem. Cycles* 24:GB3020

Sachs JP, Sachse D, Smittenberg RH, Zhang ZH, Battisti DS, Golubic S. 2009. Southward movement of the Pacific intertropical convergence zone AD 1400–1850. *Nat. Geosci.* 2:519–25

Sarmiento JL, Gruber N. 2006. *Ocean Biogecochemical Dynamics*. Princeton, NJ: Princeton Univ. Press. 502 pp.

Schneider N, Cornuelle BD. 2005. The forcing of the Pacific decadal oscillation. *J. Clim.* 18:4355–73

Shaffer G, Pizarro O, Djurfeldt L, Salinas S, Rutllant J. 1997. Circulation and low-frequency variability near the Chilean coast: remotely forced fluctuations during the 1991–92 El Niño. *J. Phys. Oceanogr.* 27:217–35

Sifeddine A, Gutierrez D, Ortlieb L, Boucher H, Velazco F, Field DB, et al. 2008. Changes in terrestrial runoff, water mass oxygenation and upwelling productivity recorded in laminated sediments off the Central Peruvian Coast spanning the last centuries. *Prog. Oceanogr.* 79:190–97

Solomon S, Rosenlof KH, Portmann RW, Daniel JS, Davis SM, et al. 2010. Contributions of stratospheric water vapor to decadal changes in the rate of global warming. *Science* 327:1219–23

Steeman-Nielsen E. 1952. The use of radioactive carbon (14C) for measuring organic production in the sea. *J. Cons. Int. Explor. Mer.* 18:117–40

Stramma L, Johnson GC, Sprintall J, Mohrholz V. 2008. Expanding oxygen-minimum zones in the tropical oceans. *Science* 320:655–58

Svendrup HW. 1953. On conditions for the vernal blooming of phytoplankton. *J. Cons. Int. Explor. Mer.* 18:287–95

Sverdrup HW, Johnson MW, Fleming RH. 1942. *The Oceans*. Englewood Cliffs, NJ: Prentice Hall

Toresen R, Østvedt OJ. 2000. Variation in abundance of Norwegian spring-spawning herring (*Clupea harengus*, Clupeidae) throughout the 20th century and the influence of climatic fluctuations. *Fish and Fisheries* 1:231–56

Annu. Rev. Marine. Sci. 2011.3:227-260. Downloaded from www.annualreviews.org
by CSIC - Consejo Superior de Investigaciones Cientificas on 11/04/11. For personal use only.

Trenberth KE, Fasullo JT. 2010. Climate change tracking earth's energy. *Science* 328:316–17
Walker GT. 1924. Correlations in seasonal variations of weather. I. A further study of world weather. *Mem. Indian Meteorol. Dep.* 111:275–332
Westberry T, Behrenfeld MJ, Siegel DA, Boss E. 2008. Carbon-based primary productivity modeling with vertically resolved photoacclimation. *Glob. Biogeochem. Cycles* 22:GB2024
Westberry TK, Siegel DA. 2006. Spatial and temporal distribution of *Trichodesmium* blooms in the world's oceans. *Glob. Biogeochem. Cycles* 20:GB4016
Whitney FA, Freeland HJ, Robert M. 2007. Persistently declining oxygen levels in the interior waters of the eastern subarctic Pacific. *Prog. Oceanogr.* 75:179–99
Williams PJL, Morris PJ, Karl DM. 2004. Net community production and metabolic balance at the oligotrophic ocean site, station ALOHA. *Deep-Sea Res.* I 51:1563–78
Winn CD, Campbell L, Christian JR, Letelier RM, Hebel DV, et al. 1995. Seasonal variability in the phytoplankton community of the North Pacific Subtropical Gyre. *Glob. Biogeochem. Cycles* 9:605–20
Wolter K, Timlin MS. 1993. *Monitoring ENSO in COADS with a seasonally adjusted principal component index*. Paper presented at 17th Clim. Diagn. Workshop, Norman, Okla.
Zachos JC, Schouten S, Bohaty S, Quattlebaum T, Sluijs A, et al. 2006. Extreme warming of mid-latitude coastal ocean during the Paleocene-Eocene Thermal Maximum: Inferences from TEX86 and isotope data. *Geology* 34:737–40
Zehr JP, Kudela RM. 2009. Photosynthesis in the open ocean. *Science* 326:945–46
Zehr JP, Paerl HW. 2008. Molecular ecological aspects of nitrogen fixation in the marine environment. In *Microbial Ecology of the Oceans*, ed. DL Kirchman, pp. 481–523. Wilmington, DE: Wiley-Liss
Zhang Y, Wallace JM, Battisti DS. 1997. ENSO-like interdecadal variability: 1900–93. *J. Clim.* 10:1004–20
Zhao M, Running SW. 2010. Drought-induced reduction in global terrestrial net primary production from 2000 through 2009. *Science* 329:940–43

Annu. Rev. Marine. Sci. 2011.3:227-260. Downloaded from www.annualreviews.org
by CSIC - Consejo Superior de Investigaciones Cientificas on 11/04/11. For personal use only.

Annual Review of
Marine Science

Volume 3, 2011

Contents

Annu. Rev. Marine. Sci. 2011.3:227-260. Downloaded from www.annualreviews.org
by CSIC - Consejo Superior de Investigaciones Cientificas on 11/04/11. For personal use only.

Errata

An online log of corrections to *Annual Review of Marine Science* articles may be found at http://marine.annualreviews.org/errata.shtml

Annu. Rev. Marine. Sci. 2011.3:227-260. Downloaded from www.annualreviews.org
by CSIC - Consejo Superior de Investigaciones Cientificas on 11/04/11. For personal use only.